ORNL/TM-7001
Dist. Category UC-20 f,g

Contract No. W-7405-eng-26

FUSION ENERGY DIVISION

A SIMPLE POWER-BALANCE MODEL FOR MICROWAVE HEATING IN EBT

D. B. Batchelor

Date Published - August 1981

Prepared by the
OAK RIDGE NATIONAL LABORATORY
Oak Ridge, Tennessee 37830
operated by
UNION CARBIDE CORPORATION
for the
DEPARTMENT OF ENERGY

CONTENTS

ABSTRACT

A simple model is presented for the production and absorption of ordinary and extraordinary mode energy in various regions of the ELMO Bumpy Torus plasma. The plasma is divided into two regions: (I) the low magnetic field side of the extraordinary mode cutoff and (II) the high field side of the cutoff. Energy balance equations are written for the sources (injection, mode conversion, and tunneling) and sinks (mode conversion, absorption, and tunneling) in each region, and simplified models are introduced to account for each of these processes. Since a typical ray makes several reflections from cavity wall surfaces before being absorbed, additional simplifying assumptions are made that the wave fields are an isotropic incoherent superposition of plane waves and that the energy density of each mode is uniform in a given region.

It is found that conversion between eigenmodes upon wall reflection and absorption of the extraordinary mode at the fundamental cyclotron resonance are the most rapid processes. The relative fractions of the injected power that is deposited in the various plasma components are typically 25% to the annulus, 22% to the core plasma, and 53% to the surface plasma. The partitioning of energy between the three plasma components is determined largely by geometric characteristics of the walls, the plasma, and the fundamental cyclotron resonant surface. The results are comparatively insensitive to other parameters of the model and in rough agreement with estimates of power deposition based on experimental data.

1. INTRODUCTION

The importance of microwave propagation and absorption in ELMO Bumpy Torus (EBT) cannot be overemphasized in that plasma production, heating, and stabilization by means of the hot electron annuli are dependent on these processes. A quantitative understanding of microwave energy deposition in the core plasma is, of course, necessary to interpret experimental energy confinement studies in the current devices. Also, a knowledge of microwave propagation and absorption processes is necessary in order to extrapolate with any confidence to larger EBT devices such as EBT-P and an EBT reactor.

In the present work we concentrate on modeling the EBT-I device. In the EBT-I experiment three different plasma components are observed (see Fig. 1): (1) an annular, high beta, relativistic electron component, which is mirror-confined in each sector; (2) a toroidally circulating, isotropic core component of moderate density and temperature, which is radially confined inside the magnetic well produced by the annulus; and (3) a cold, low density surface plasma extending from the outer edge of the annulus to the cavity wall. A major result of the power balance model has been to provide estimates of the total microwave power deposited in each of the plasma components.

A number of theoretical studies [1-3] have been undertaken to elucidate the role of various propagation and absorption processes in EBT, and a qualitative understanding has been obtained, at least of the core heating in EBT-I. For the complicated, asymmetrical geometry of EBT, details of the wave propagation characteristics and absorption must be determined by ray tracing. However, some general statements can be made:

- A central feature of the propagation is the presence of the extraordinary mode, right-hand cutoff. This evanescent zone prevents extraordinary mode energy injected near the mirror midplane from propagating directly to the fundamental cyclotron resonance.
- Because of strong gradients in $|\underline{B}|$ along field lines, any extraordinary mode energy propagating from the high field side (mirror throat region) is totally absorbed at the fundamental resonance. This is true even for the low density surface plasma.
- The density and temperature of the core plasma in EBT-I are sufficiently small that heating of the core plasma by the ordinary mode is negligible at both the fundamental and second harmonic resonance.
- Heating of the core plasma by the extraordinary mode is negligible at the second harmonic resonance.
- Both ordinary and extraordinary modes are absorbed by the hot electron annuli. Experimental measurements of the annulus energy lifetime indicate that one-fourth to one-third of the total injected power is absorbed by the annuli.
- Plasma resonance occurs at the upper hybrid frequency only for perpendicularly stratified plasmas. Because of the geometry of EBT, the upper hybrid resonance plays no role.

Since the core plasma in EBT-I is observed to be strongly heated, some mechanism must exist whereby extraordinary mode energy reaches the high magnetic field region, from which it can be efficiently absorbed at the fundamental cyclotron resonance. A number of mechanisms have

been considered in this regard, including Budden tunneling, destruction of the cutoff by finite temperature effects, and depolarization of ordinary mode energy into extraordinary mode in the high field region upon wall reflection. Of these, the dominant process appears to be conversion of ordinary mode energy to extraordinary mode in the high field region. In considering a low density, magnetized plasma having parameters characteristic of the surface plasma in EBT-I in contact with a perfectly conducting wall, it is found that a fraction of ordinary mode approaching 100% is converted to extraordinary mode for certain angles of incidence on the wall. Averaging over a uniform distribution in the angle of incidence gives average conversion efficiencies in the vicinity of 50% for parameters characteristc of the mirror throat region in EBT-I.

The core heating of EBT-I can be summarized as follows. Extraordinary mode energy injected at the midplane is partially absorbed by the annulus, partially depolarized into ordinary mode upon wall reflection, and weakly absorbed and transmitted to the high field region by Budden tunneling. Aside from these sinks, extraordinary mode energy is trapped in the region outside the right-hand cutoff. Ordinary mode energy launched from the midplane is partially absorbed by the annulus and partially depolarized into extraordinary mode at all wall surfaces, but it is only weakly absorbed by the core plasma. Any extraordinary mode energy produced in the high field mirror throat region or tunneling through to the high field region is strongly absorbed at the fundamental cyclotron resonance.

It has proved very difficult to make detailed calculations of the radial heat deposition profiles using geometrical optics. This is because the production of extraordinary mode energy in the high field region is such an indirect process involving mode conversion and Budden tunneling (which are manifestations of a breakdown in the geometrical optics model) and because each ray (either ordinary or extraordinary mode) typically experiences several reflections and transits across the irregularly shaped EBT cavity before its energy is completely deposited. After a few reflections the direction of propagation and rate of energy absorption become a very sensitive, nearly random function of the ray's initial conditions. The calculation of heating profiles by detailed ray tracing therefore carries with it much of the futility of doing statistical mechanics as an initial value problem.

In the present model we do not attempt to calculate the complete radial heating profile. Rather, we divide the plasma in each EBT sector into two regions (see Fig. 1). Region I is that region near the midplane which is on the low magnetic field side (the propagating side) of the right-hand cutoff. Region II contains all plasma at a magnetic field higher than the cutoff. Considering the different propagation characteristics, energy sources, and energy sinks for ordinary and extraordinary mode in the two regions, we can estimate certain gross heating features, such as the power deposited in the core, the annulus and surface plasmas, the total electromagnetic stored energy in each mode, and cavity Q.

Advantage is taken of the multiple reflections experienced by the rays to make the assumptions that the radiation in each mode is

isotropically propagating and that the energy density is uniform in each region. In order to make progress, we adopt highly simplified models for the wave absorption and mode conversion processes. Obviously, the results of the model are only approximate and should be viewed with the same degree of confidence as zero-dimensional transport models. However, we have found this model to be of value in exhibiting trends and in showing sensitivities to the various assumptions on propagation and absorption models.

In Section 2 the power balance model is presented, and simplified equations are derived relating the energy density in the different wave modes to the input power and to rate coefficients for the various absorption and conversion processes. In Section 3, the various absorption models and absorption rate coefficients are discussed. The effects of Budden tunneling and absorption are discussed in Section 4. An extensive discussion of the process whereby one plasma eigenmode is converted to another upon wall reflection is presented in Section 5. The magnitudes of the various rate coefficients all depend on geometric characteristics of the device, such as the areas of the resonance surfaces. In Section 6, the geometric parameters used in the calculations are presented and estimates are given for the rate coefficients. In Section 7, results of calculations using the model are discussed.

2. POWER BALANCE MODEL

For any region V bounded by a surface S, energy conservation for the jth wave mode can be written

$$P_j - A_j - \sum_k T_{jk} + \sum_k T_{kj} = 0 \tag{2.1}$$

where

$$P_j = \int_S d\underset{\sim}{\sigma} \int_{\underset{\sim}{k}\ \text{incident}} d^3k\ \underset{\sim}{s}^j(\underset{\sim}{x},\underset{\sim}{k}) = \text{jth mode power flowing into V}$$

$$A_j = \int_V d^3x \int_{\underset{\sim}{k}\ \text{incident}} d^3k\ \underset{\sim}{E}^j(\underset{\sim}{x},\underset{\sim}{k})^* \cdot \underset{\approx}{\sigma}^H(\underset{\sim}{x},\underset{\sim}{k}) \cdot \underset{\sim}{E}_j(\underset{\sim}{x},\underset{\sim}{k}) = \text{power dissipated from jth mode throughout V}$$

and

$$T_{jk} = \int_{S_C} d\underset{\sim}{\sigma} \int_{\underset{\sim}{k}\ \text{incident}} d^3k\ t_{jk}(\underset{\sim}{x},\underset{\sim}{k})\underset{\sim}{s}^j(\underset{\sim}{x},\underset{\sim}{k}) = \text{power in jth mode converted to kth mode at conversion surface } S_C \text{ with}$$

$\underset{\sim}{s}^j(\underset{\sim}{x},\underset{\sim}{k})$ = Poynting flux

$\underset{\approx}{\sigma}^H(\underset{\sim}{x},\underset{\sim}{k})$ = Hermitian part of the plasma conductivity tensor and

$t_{jk}(\underset{\sim}{x},t)$ = mode conversion coefficient

As written, the power absorption is a volume effect. In fact, for the cyclotron fundamental, the absorption takes place in a thin region near the resonant surface so that A_j can reasonably be modeled as

$$A_j = \int_{S_R} d\underset{\sim}{\sigma} \int_{\underset{\sim}{k}\ \text{incident}} d^3k \alpha_j(\underset{\sim}{x},\underset{\sim}{k}) \underset{\sim}{s}^j(\underset{\sim}{x},\underset{\sim}{k}) = \text{power dissipated} \qquad (2.2)$$

from jth mode at resonant absorption surface S_R

where $\alpha_j(\underset{\sim}{x},\underset{\sim}{k})$ = fractional absorption coefficient.

All terms in Eq. (2.1) have now been related to the power flux $\underset{\sim}{s}_i^j$ incident on some surface. Since each ray undergoes a number of reflections on the average before being absorbed, we adopt the assumption that the microwave field consists of an isotropic superposition of plane waves. The Poynting flux, per unit solid angle about the group velocity $\underset{\sim}{v}_g$, can be related to the wave energy density in the jth mode, W_j, and the group velocity $\underset{\sim}{v}_g$ according to

$$\underset{\sim}{s}^j(\underset{\sim}{x},\underset{\sim}{k}) = \frac{|\underset{\sim}{s}^j(\underset{\sim}{x})|}{4\pi} \hat{v}_g(\underset{\sim}{k}) = \frac{\underset{\sim}{v}_g(\underset{\sim}{k})}{4\pi} W_j(\underset{\sim}{x}) \qquad (2.3)$$

where, for simplicity, we usually assume $|\underset{\sim}{v}_g| = c$ and take the direction of energy propagation $\hat{v}_g$ to be in the direction of $\underset{\sim}{k}$. By making the further simplifying assumption that the energy density is constant throughout each of the plasma regions, $W_j(\underset{\sim}{x}) = W_j^{I,II}$ = constant, the energy density can be taken outside the integrals over $d\underset{\sim}{\sigma}$ and $d^3\underset{\sim}{k}$. For example,

$$A_X^I = W_X^I \int_{S_R} d\underset{\sim}{\sigma} \int_{\underset{\sim}{k}\ \text{incident}} 4\pi\alpha_X(\underset{\sim}{x},\underset{\sim}{k})\underset{\sim}{v}_g = \text{extraordinary mode} \qquad (2.4)$$

power dissipated in region I

This can ultimately be written as the product of the energy density with the dissipation rate coefficient averaged over the resonant surface

and the angle of incidence

$$A_X^I = \alpha_X^I W_X^I \tag{2.5}$$

where

$$\alpha_X^I = \int_{S_R^I} d\underset{\sim}{\sigma} \int_{\underset{\sim}{k} \text{ incident}} \frac{d^3k}{4\pi} \underset{\sim}{v}_g(\underset{\sim}{k}) \alpha_X(\underset{\sim}{x},\underset{\sim}{k})$$

and S_R^I is all cyclotron resonant surfaces in region I. (In the case of region I, this is the second harmonic resonance.)

Similar expressions can be written for the mode conversion terms; for example,

$$T_{XO}^I = W_X^I \int_{S_C^I} d\underset{\sim}{\sigma} \int \frac{d^3k}{4\pi} \underset{\sim}{v}_g(\underset{\sim}{k}) t_{XO}(\underset{\sim}{x},\underset{\sim}{k}) \equiv \tau_{XO}^I W_X^I \tag{2.6}$$

= extraordinary mode power converted to ordinary mode

in region I where S_C^I is the mode conversion surface in region I and τ_{XO}^I is the average (over the wall surface and the angle of incidence) rate of mode conversion. In this way we obtain equations for the ordinary and extraordinary mode power densities in each of the two regions. For example, the equation for extraordinary mode energy density in region I can be written

$$P_X - \alpha_X^I W_X^I - \tau_{XO}^I W_X^I + \tau_{OX}^I W_O^I - (\gamma_A + \gamma_T) W_X^I = 0 \tag{2.7}$$

where

P_X = extraordinary mode power injected from the waveguide

W_X^I = extraordinary mode energy density in region I

W_O^I = ordinary mode energy density in region I

$\alpha_X^I W_X^I$ = extraordinary mode power absorbed in region I (i.e., the annulus absorption in EBT-I)

$\tau_{XO}^I W_X^I$ = extraordinary mode power converted to ordinary mode in region I

$\tau_{OX}^I W_O$ = ordinary mode power converted to extraordinary mode in region I

$\gamma_A W_X^I$ = extraordinary mode power absorbed by Budden tunneling

$\gamma_T W_X^I$ = extraordinary mode power transmitted to region II by Budden tunneling

For the extraordinary mode in region II we obtain

$$\gamma_T W_X^I - \alpha_X^{II} W_X^{II} - \tau_{XO}^{II} W_X^{II} + \tau_{OX}^{II} W_O^{II} = 0 \qquad (2.8)$$

Since the ordinary mode is not cut off anywhere in the plasma, we expect that $W_O^I = W_O^{II} \equiv W_O$ and obtain a single equation for ordinary mode power balance:

$$P_O = (\alpha_O^I + \alpha_O^{II}) W_O - (\tau_{OX}^I + \tau_{OX}^{II}) W_O + \tau_{XO}^I W_X^I + \tau_{XO}^{II} W_X^{II} = 0 \qquad (2.9)$$

where

P_O = ordinary mode power injected from waveguide

$\alpha_O^N W_O$ = power dissipated directly from ordinary mode in region N

3. ABSORPTION MODELING

In order to proceed, it is necessary to calculate the absorption, tunneling, and mode conversion coefficients α, τ, and γ. Absorption of extraordinary mode energy in the high field region can be modeled quite simply. Ray-tracing studies [1] show that in a plasma with strong gradients in $|\underset{\sim}{B}|$ along field lines (when extraordinary mode waves approach cyclotron resonance from the high magnetic field side), $k_{\parallel}$ becomes large, and the damping is very strong, provided $\omega_{pe}^2/\Omega_e^2 \times c/v_e \gtrsim 1$. This condition is satisfied all along the $\Omega_e = \omega$ layer in EBT even for the low density surface plasma. We therefore assume that all extraordinary mode energy incident on the resonance surface from the high field side is absorbed. Taking $\underset{\sim}{v}_g = c\hat{\underset{\sim}{k}}$ and $\alpha_x(\underset{\sim}{x},\underset{\sim}{k}) = 1$ and introducing the unit normal to the resonant surface $\hat{n}$, α_x^{II} can be expressed as [see Eq. (2.5)]

$$\alpha_X^{II} = c \int_{S_R^{II}} d\sigma \int \frac{d\Omega}{4\pi} \hat{k} \cdot \hat{n} = \frac{c}{2} \int_{S_R^{I}} d\sigma = \frac{c}{2} S_R^{II} \tag{3.1}$$

where S_R^{II} is the total area of the fundamental resonant surface. Later, it will be convenient to divide the fundamental resonance surface into two parts (see Fig. 1): S_C^{II} = that part of the resonance surface which intercepts the core plasma component, and S_S^{II} = the remainder of the resonant surface which intercepts the surface plasma. The extraordinary mode power deposited in the core plasma component from the high field side is therefore $\frac{c}{2} S_C^{II} W_X^{II}$, whereas $\frac{c}{2} S_S^{II} W_X^{II}$ is the power deposited in the surface component.

Ray-tracing studies [1,4] have shown that the ordinary mode is only very weakly damped at the fundamental cyclotron resonance in EBT-I. Typical fractions of power absorbed for ordinary mode rays passing through resonance are less than a few percent. We can make this result more quantitative by averaging over an assumed isotropic distribution of incident ordinary mode rays.

We consider the plasma near the fundamental resonance to be plane stratified in the direction parallel to the magnetic field lines; i.e., $\underset{\sim}{B}(\underset{\sim}{x}) = [0,0,B_0(1 + z/L)]$. Choosing the resonance at $z = 0$, the cyclotron frequency can be written $\Omega_e = \omega[1 + (z/L)]$ where ω is the wave frequency. Using Eq. (29) of Ref. [3], the imaginary part of the refractive index n_i in the direction of the group velocity can be written

$$n_i \equiv \mathrm{Im}\left\{\frac{\underset{\sim}{n}\cdot\underset{\sim}{s}}{|\underset{\sim}{s}|}\right\} = -\frac{n_\perp^2(1 - n^2 - 2P)^2}{4n_\parallel}\frac{|E_\parallel|^2}{4\pi|\underset{\sim}{s}|}\frac{1}{P}\frac{v_e}{c}\,\mathrm{Im}\left\{\frac{1}{Z(\xi)}\right\} \qquad (3.2)$$

where

$\underset{\sim}{n} = \dfrac{c\underset{\sim}{k}}{\omega}$ = refractive index

$\underset{\sim}{s}$ = Poynting vector

$P = \dfrac{\omega_{pe}^2}{\Omega_e^2}$

$E_\parallel$ = parallel component of the wave field

$Z(\xi)$ = plasma dispersion function

$\xi = \dfrac{\omega - \Omega_e(z)}{k_\parallel v_e} = \dfrac{c}{v_e}\dfrac{1}{n_\parallel}\dfrac{z}{L}$

The real part of the refractive index is given by the zero-order dispersion relation

$$n_{\pm}^2 = \frac{2(1 - P) + \sin^2\theta \pm \{[2(1 - P) + \sin^2\theta]^2 - 4(1 - P)(2 - P)\sin^2\theta\}^{1/2}}{2 \sin^2\theta} \tag{3.3}$$

where + and - refer to the extraordinary and ordinary modes, respectively.

The fraction of power absorbed from a ray in passing through resonance f is given by

$$f = \exp[-2\ \omega/c \int_{-\infty}^{\infty} ds\ n_i(s)] \equiv \exp(-2\alpha) \tag{3.4}$$

where s is the arc length along the ray. For the parallel stratified geometry considered here we have

$$\int ds\ n_i(s) = \int dz \frac{ds}{dz} n_i(z) = \int dz \frac{|\underset{\sim}{s}|}{s_z} n_i(z)$$

so that α as defined in Eq. (3.4) can be expressed

$$\alpha = -\frac{\omega}{c} \int_{-\infty}^{\infty} dz \frac{n_\perp^2(1 - n^2 - 2P)^2}{4n_\parallel} \frac{|E_\parallel|^2}{4\pi s_z} \frac{1}{P} \frac{v_e}{c} \mathrm{Im}\left\{\frac{1}{Z\left(\frac{c}{n_\parallel v_e} \frac{z}{L}\right)}\right\} \tag{3.5}$$

Using the equations

$$s_z = \frac{1}{4\pi} \frac{|E_\parallel|^2}{n_\perp^2 n_\parallel} (1 - n_\perp^2 - P)(2 - n_\perp^2 - 2P)$$

and

$$\int_{-\infty}^{\infty} dz\ \mathrm{Im}\left\{\frac{1}{Z\left(\frac{c}{n_{\parallel} v_e}\frac{z}{L}\right)}\right\} = -\pi\ \frac{n_{\parallel} v_e}{2c}$$

we finally obtain

$$\alpha = \frac{\omega}{c}\frac{\pi}{8} n_{\parallel}\ \frac{L}{P}\left(\frac{v_e}{c}\right)^2\ \frac{n_{\perp}^4 (1 - n^2 - 2P)^2}{(1 - n_{\perp}^2 - P)(2 - n_{\perp}^2 - 2P)} \tag{3.6}$$

To obtain the average fractional absorption we numerically compute the integral

$$\langle f \rangle = \frac{1}{4\pi} \int d\phi\ \sin\psi\ d\psi\ f(\psi) = \int_0^{\pi/2} d\psi\ \sin\psi\ f(\psi) \tag{3.7}$$

where ϕ is the azimuthal and ψ is the angle between $\underset{\sim}{v}_g$ and $\underset{\sim}{B}$.

Figure 2 shows f as a function of $n_{\perp}$ for various values of P and for the case f_{μ} = 18 GHz, L = 10 cm, which is appropriate for EBT-I. Also shown is <f> obtained from Eq. (3.7) for each value of P. It can be seen that even for the highest plausible densities in EBT-I the absorption is less than a few percent for most angles. There are very sharp peaks near the values of $n_{\perp}$ for which the wave vector is perpendicular to the magnetic field. Near perpendicular propagation the absorption exponent a diverges [$n_{\parallel}^2 \propto (1 - n_{\perp}^2 - P)$ so $n_{\parallel}/(1 - n_{\perp}^2 - P) \to 1/n_{\parallel}$ as $n_{\parallel} \to 0$]. This is because in nonrelativistic theory the ordinary mode damping rate becomes large as $n_{\parallel} \to 0$ and because the length of the ray lying in the resonant zone becomes infinite as $\psi \to \pi/2$. Since the

resonant zone in EBT is curved rather than straight (as in this plane stratified model) and is of finite extent, a ray cannot actually remain in the resonant zone for a distance larger than about L. In view of the approximate nature of the power balance model, we have not attempted to refine this analysis by including relativistic effects for propagation angles near 90° or by introducing a cutoff in ψ to limit the length of the ray. We regard the results shown in Fig. 2 as very conservative overestimates of the ordinary mode absorption at the fundamental resonance. This therefore verifies, using a continuous distribution of rays, the findings of ray-tracing studies that the ordinary mode absorption is less than a few percent in EBT-I.

The model we have adopted for ordinary mode absorption at the fundamental resonance takes the form

$$\alpha_O^{II} = c\langle f\rangle \int_{S_R^{II}} d\sigma \int \frac{d\Omega}{4\pi}\, \hat{k} \cdot \hat{n} = c\langle f\rangle S_C^{II} \tag{3.8}$$

where $\langle f\rangle$ is chosen in the range 0.0-0.05. The integral over the solid angle is taken as a full 4π since both sides of the resonant zone are accessible to the ordinary mode.

Modeling of wave absorption in region I (i.e., absorption at the second harmonic resonance by the hot electron annulus) is a much more difficult task. The calculation of wave absorption properties of the annulus requires the analysis of a fully relativistic dispersion relation. This analysis is in progress, but only preliminary results are available as yet. A concern in this regard arises from the annulus parameters: $v_e/c \sim 1$, $k_\perp \rho_e \sim 1$, and $k_\perp L_A \sim 1$ where L_A is a spatial scale length for

variations in annulus parameters. The geometrical optics approach therefore may not be meaningful. In addition, the geometric and plasma parameters of the annulus are not yet accurately known. The best presently available information concerning the microwave power absorbed by the annulus is obtained from observations of the plasma stored energy and the energy lifetime in power turn-down experiments [5]. From these experiments one estimates that a fraction between 0.2 and 0.3 of the power deposited in the plasma goes into the annulus.

We have adopted a model in which the extraordinary mode and ordinary mode absorption in region I are of the form

$$\alpha_X^I = g_X \alpha_A \ , \quad \alpha_O^I = (1 - g_X)\alpha_A \ , \quad 0 \leq g_X \leq 1 \tag{3.9}$$

where α_A is an overall annulus absorption coefficient and g_X measures the relative opacity of the annulus to extraordinary mode waves compared to ordinary mode. The total power absorbed by the annulus is then

$$P_A = \alpha_A [g_X W_X^I + (1 - g_X) W_O] \tag{3.10}$$

At nonrelativistic temperatures the absorption of ordinary mode radiation at the second harmonic resonance is much weaker than extraordinary mode absorption. At higher temperatures the second harmonic absorption rates begin to equalize. However, for temperatures in the range 100-200 keV, which are relevant for EBT-I, the extraordinary mode absorption is still 4-5 times as great as that for the ordinary mode. The most likely range for g_X is therefore $0.8 \lesssim g_X \leq 1.0$. The widest conceivable range is $0.5 \leq g_X \leq 1.0$.

We begin by treating α_A as an unknown to be determined by constraining P_A to be some fixed fraction of the total input power P_{TOT} (typically $P_A/P_{TOT} = 0.25$). We can then determine the sensitivity of the results to various values of the other modeling parameters. In other cases we have fixed α_A such that $P_{ANNULUS} = 0.25P_{TOT}$ for one set of parameters and then determined the variation of $P_{ANNULUS}$ as the parameters changed.

We have also used the initial results of the relativisitic absorption calculations to construct a simple a priori model for annulus absorption. The annulus in EBT-I is observed to form at the location of the vacuum second harmonic cyclotron resonance (this is at a radius of 10-12 cm). The axial length of the annulus is estimated to be approximately equal to its radius. The thickness is about 4 cm. Fully relativistic calculations of absorption using a two-dimensional (2-D) finite-beta model for the annulus and using plasma parameters appropriate for EBT-I [6] have shown that a maximum of about 33% of the power in the extraordinary mode ray is absorbed in a single pass through the annulus. Assuming an isotropic flux of rays incident on the edge of the annulus at the midplane, we find a rough average over the solid angle and axial position of power absorbed from a ray in a single pass is $\langle f \rangle_A \cong 0.12\text{-}0.15$. We treat the annulus as a cylindrical surface of radius $r_A \sim 11$ cm and length $L_A \sim 11$ cm and assume that a fraction $\langle f \rangle_A$ of the power is absorbed when a ray intersects the surface. The overall absorption coefficient is then modeled:

$$\alpha_A = 2\pi c r_A L_A \langle f \rangle_A \cong 2.9 \times 10^{12} \text{ cm}^3/\text{s}$$

where we have taken $\langle f \rangle_A = 0.13$.

4. TUNNELING MODEL

Since the evanescent zone between the extraordinary mode cutoff and the cyclotron resonance layer is thin in the low density surface plasma region, the possibility exists for extraordinary mode energy to tunnel through to the cyclotron resonance layer and to be partially transmitted to the high field region. An analysis of Budden tunneling of obliquely propagating extraordinary mode waves in parallel stratified plasmas shows [2] that for the case $\omega/cL_z << 1$ and $n_\perp^2 << 1$ (L_z is magnetic field gradient scale length and $n_\perp$ is the refractive index perpendicular to $\underset{\sim}{B}$) the energy absorption coefficient $|A|^2$ and the transmission coefficient $|T|^2$ are:

$$|A|^2 = \exp(-\pi K_0 X_0)[1 - \exp(-\pi K_0 X_0)]$$

$$|T|^2 = \exp(-\pi K_0 X_0) \tag{4.1}$$

where

$$K_0^2 = \frac{\omega^2}{c^2}\left[1 - \frac{(2 - P)n_\perp^2}{2(1 - P)}\right]$$

$$X_0 = L_z P\left[1 - \frac{(1 - P)n_\perp^2}{2(1 - P) - n_\perp^2}\right]^{-1}$$

$$P = \frac{\omega_{pe}^2}{\Omega_e^2}$$

Expanding for small P appropriate to the surface plasma we find

$$K_0 X_0 \cong \frac{\omega}{c} L_z P \left[1 - \frac{P n_\perp^2}{4(1 - P)}\right] \tag{4.2}$$

The first term is the limiting result for propagation parallel to the magnetic field, whereas the second term is a correction for oblique propagation. For the small values of P encountered in the surface plasma, $P \sim 0.025\text{-}0.05$ ($\Omega_e/2\pi = 18$ GHz, $n_e \sim 1\text{-}2 \times 10^{11}/\text{cm}^3$), the correction is indeed small. Numerical integration of the field equations [2] shows that Eq. (4.1) is actually valid for comparatively large $n_\perp$ ($n_\perp \sim 0.5$). For larger $n_\perp$, even though the approximation $n_\perp^2 << 1$ breaks down, the expressions for $|A|^2$ and $|T|^2$ are approximately correct. The breakdown in the formalism is manifested in partial conversion of the incident extraordinary mode energy to ordinary mode.

Assuming a magnetic field scale length $L_z \sim 6.5$ cm and P values as mentioned above, one obtains for the lowest densities $|T|^2 \sim 0.15$, $|A|^2 \sim 0.125$ and for the higher densities $|T|^2 \sim |A|^2 \sim 0.01$. To model the tunneling in the power balance equations we assume that any extraordinary mode wave incident on the cutoff-resonance surface from region I is transmitted to region II with efficiency $|T|^2$. Therefore, the total power transmitted to region II is $\gamma_T W_X^I$ where

$$\gamma_T = |T|^2 \frac{c}{2} S_S^{II} \tag{4.3}$$

Similarly, the extraordinary mode power dissipated from region I by means of Budden tunneling is $\gamma_A W_X^I$ where

$$\gamma_A = |A|^2 \frac{c}{2} S_S^{II}$$

and (4.4)

$$|A|^2 = |T|^2(1 - |T|^2)$$

In the calculations we have examined the consequences of allowing $|T|^2$ to range from 0 to 0.15, which seems to be the credible range.

5. MODE CONVERSION

Another process that is important in establishing the power balance in EBT is conversion of one wave mode to the other upon reflection or scattering by a conducting wall surface. When, for example, an ordinary mode wave in a magnetized plasma is incident on a perfectly conducting surface in contact with the plasma, a significant amount of power in the reflected wave is in the extraordinary mode, depending on plasma density, magnetic field, and angle of incidence.

Consider the wave depolarization situation diagrammed in Fig. 3. A cold plasma of constant density is in contact with the conducting surface in the x-y plane, and a uniform magnetic field $\underset{\sim}{B}$ is in the x-z plane making an angle ψ with respect to the z-axis. A wave of pure characteristic mode (for example, ordinary mode) is incident from above with refractive index $\underset{\sim}{n}^{O}$ where n_x, n_y are specified and n_z^O is determined from the Booker quartic equation. As a result of Snell's law, n_x, n_y are conserved for the reflected wave, but $n_z = n_z^{O'}$ is, in general, different from n_z^O of the incident wave. Also, the electric field eigenvector $\underset{\sim}{E}^{O'}$ is different from the electric field of the incident ordinary mode wave $\underset{\sim}{E}^{O}$. In order to enforce the boundary condition that the transverse component of the electric field vanish at the surface, it is necessary that a component of the extraordinary mode $\underset{\sim}{E}^{X'}$ be included in the reflected wave.

For the configuration diagrammed in Fig. 3, the electric fields are determined from the dielectric tensor

$$\underset{\approx}{D} \cdot \underset{\sim}{E} = 0 \tag{5.1}$$

where

$$\underset{\approx}{D}(n_z) =$$

$$\begin{bmatrix} 1 - P\dfrac{1 - b_x^2}{1 - b^2} - n_y^2 - n_z^2 & \dfrac{-iPb_z}{1 - b^2} + n_x n_y & \dfrac{Pb_x b_y}{1 - b^2} + n_x n_z \\ \dfrac{iPb_z}{1 - b^2} + n_x n_y & 1 - \dfrac{P}{1 - b^2} - n_x^2 - n_z^2 & \dfrac{-iPb_x}{1 - b^2} + n_y n_z \\ \dfrac{Pb_x b_z}{1 - b^2} + n_x n_z & \dfrac{iPb_x}{1 - b^2} + n_y n_z & 1 - P\dfrac{1 - b_z^2}{1 - b^2} - n_x^2 - n_y^2 \end{bmatrix}$$

where

$$P = \frac{\omega_{pe}^2}{\omega^2}$$

$$b = \frac{|\Omega_e|}{\omega}$$

$$\underset{\sim}{n} = \frac{c}{\omega}\underset{\sim}{k}$$

$$b_x = \frac{B_x}{B}\frac{|\Omega_e|}{\omega} = b \sin \psi$$

$$b_z = \frac{B_z}{B}\frac{|\Omega_e|}{\omega} = b \cos \psi$$

For given n_x, n_y, and ψ, the condition for Eq. (5.1) to have nontrivial solutions is that n_z satisfy the dispersion relation, which can be expressed in the present notation as

$$An_z^4 + Bn_z^3 + Cn_z^2 + Dn_z + E = 0 \tag{5.2}$$

where

$$A = 1 - P - b^2 + Pb_z^2$$

$$B = 2Pb_x b_z n_x$$

$$C = -2(1 - P - b^2)(1 - n_\parallel^2 - P) + P(b_x^2 + b_z^2 n_\parallel^2 + b_x^2 n_x^2)$$

$$D = -2(1 - n_\parallel^2) n_x P b_x b_z$$

$$E = (1 - P)(1 - n_\parallel^2 - P)^2 - (1 - n_\parallel^2)(1 - n_\parallel^2 - P)b^2 - (1 - n_\parallel^2) n_x^2 P b_x^2$$

This is equivalent to the Booker quartic equation [6]. We assume that all four roots of Eq. (5.2) are real. For the low densities of interest in the surface region of EBT ($P \ll 1$), this is satisfied for most values of n_x, n_y. It can then be shown that two of the roots are upgoing waves, $n_z > 0$, while two are downgoing, $n_z < 0$. Also, for $P < 1$ one of the upgoing and one of the downgoing waves can be associated with the ordinary mode and, similarly, for the extraordinary mode. We therefore enumerate the roots of Eq. (5.2), n_z^j, as follows:

$n_z^1 \Rightarrow$ downgoing ordinary mode

$n_z^2 \Rightarrow$ downgoing extraordinary mode

$n_z^3 \Rightarrow$ upgoing ordinary mode

$n_z^4 \Rightarrow$ upgoing extraordinary mode

The correspondence between n_z^j and ordinary/extraordinary modes is made by calculating θ, the angle between $\underset{\sim}{B}$ and $\underset{\sim}{n}^j = (n_x, n_y, n_z^j)$, and by comparing $\underset{\sim}{n}^j \cdot \underset{\sim}{n}^j$ to the Appleton-Hartree dispersion relation.

Once the correct roots have been determined, the associated polarization eigenvectors $\underset{\sim}{E}^j$ can be found from the dispersion tensor by solving

$$\underset{\approx}{D}(n_z^j) \cdot \underset{\sim}{E}^j = 0 \qquad (5.3)$$

Assuming an incident downgoing ordinary mode wave j = 1, the reflected wave is a linear combination of upgoing ordinary and extraordinary mode waves: $\underset{\sim}{E}_{\text{reflected}} = C_{OO}\underset{\sim}{E}^3 + C_{OX}\underset{\sim}{E}^4$. The boundary condition at the conducting surface is that the tangential electric field vanish:

$$\begin{aligned} E_x^1 + C_{OO}E_x^3 + C_{OX}E_x^4 &= 0 \\ E_y^1 + C_{OO}E_y^3 + C_{OX}E_y^4 &= 0 \end{aligned} \tag{5.4}$$

Similarly, if the incident wave is a downgoing extraordinary mode j = 2, the reflected wave can be written as the linear combination $\underset{\sim}{E}_{\text{reflected}} = C_{XO}\underset{\sim}{E}^3 + C_{XX}\underset{\sim}{E}^4$, and the boundary conditions give the equations

$$\begin{aligned} E_x^2 + C_{XO}E_x^3 + C_{XX}E_x^4 &= 0 \\ E_y^2 + C_{XO}E_y^3 + C_{XX}E_y^4 &= 0 \end{aligned} \tag{5.5}$$

Equations (5.4) and (5.5) are then solved for the amplitude conversion coefficients C_{ij}.

In order to calculate the power in each reflected mode, it is necessary to evaluate the Poynting flux $\underset{\sim}{s}^i$ carried by each eigenvector $\underset{\sim}{s}^i = \text{Re}\{\underset{\sim}{E}^i \times \underset{\sim}{B}^{i*}\}/8\pi$. In particular, the power flux in the z direction is given by

$$s_z^i = \frac{1}{8\pi}\,\text{Re}\{n_z^i|E^i|^2 - (\underset{\sim}{n}^i \cdot \underset{\sim}{E}^i)E_z^{i*}\} \tag{5.6}$$

The power in the ith mode converted to jth mode upon reflection can therefore be conveniently expressed in matrix form T_{ij} as

$$\underset{\approx}{T} = \begin{bmatrix} |C_{OO}|^2 \frac{S_z^3}{S_z^1} & |C_{XO}|^2 \frac{S_z^3}{S_z^2} \\ |C_{OX}|^2 \frac{S_z^4}{S_z^1} & |C_{XX}|^2 \frac{S_z^4}{S_z^2} \end{bmatrix} \tag{5.7}$$

Numerical calculations of $\underset{\approx}{T}$ for all angles of incidence have confirmed certain properties that were expected, such as symmetry ($T_{OX} = T_{XO}$ and $T_{OO} = T_{XX}$) and energy conservation ($T_{OO} + T_{OX} = T_{XX} + T_{XO} = 1$).

We first briefly consider the much simplified case in which $n_y = 0$ and $\psi = 90°$ [i.e., $\underset{\sim}{B} = (B,0,0)$]. With these assumptions the dispersion tensor reduces to

$$\underset{\approx}{D}(n_z) = \begin{bmatrix} 1 - P - n_z^2 & 0 & n_x n_z \\ 0 & 1 - \varepsilon - n^2 & -ib\varepsilon \\ n_x n_z & ib\varepsilon & 1 - \varepsilon - n_x^2 \end{bmatrix} \tag{5.8}$$

where $\varepsilon = P/(1 - b^2)$. The dispersion relation [Eq. (5.2)] reduces to a quadratic equation in n_z^2 whose roots at low density ($P < 1$) can be associated with the ordinary and extraordinary modes as follows:

$$\left.\begin{matrix} n_X^2 \\ n_O^2 \end{matrix}\right\} = -\frac{C \pm \sqrt{\Delta}}{2E} \tag{5.9}$$

where Δ is the discriminant of the quadratic equation obtained from Eq. (5.2) in the limit $b_x \to 0$, $n_y \to 0$. Taking n_X and n_O as positive square roots of the above expressions we have (according to the previous enumeration of roots)

$$n_z^1 = -n_O \ , \quad n_z^2 = -n_X \ , \quad n_z^3 = +n_O \ , \quad n_z^4 = +n_X$$

The electric field eigenvectors $\underset{\sim}{E}^j$ can be obtained by direct inspection of Eq. (5.8)

$$\underset{\sim}{E}^j = \left(- \frac{n_z n_x^j}{1 - P - n_z^{j2}} \ , \quad i \frac{b\varepsilon}{1 - \varepsilon - n^2} \ , \quad 1 \right) \tag{5.10}$$

valid for $n_z^j \neq 0$, $n_x \neq 0$. Notice that the upgoing and downgoing eigenvectors of a given mode are identical except for the sign of E_x^j. Obviously, the upgoing and downgoing eigenvectors are linearly independent so that some coupling must occur unless n_z^j or n_x vanishes. In this limit it is also easy to calculate the Poynting flux

$$\underset{\sim}{S}^j = \frac{1}{8\pi} \left[n_z^j (|E_x^j|^2 + |E_y^j|^2) - n_x E_x E_z^* \right] \tag{5.11}$$

Solving Eq. (5.4) for C_{OX} and using $\underset{\sim}{E}^j$ as given by Eq. (5.10), we obtain for the conversion coefficient

$$T_{OX} = 4 \frac{n_X}{n_O} \left[\frac{\dfrac{(1 - P) n_x^2}{(1 - P - n_X^2)^2} + \dfrac{b^2 \varepsilon^2}{(1 - \varepsilon - n_x^2 - n_X^2)^2}}{\dfrac{(1 - P) n_x^2}{(1 - P - n_O^2)^2} + \dfrac{b^2 \varepsilon^2}{(1 - \varepsilon - n_x^2 - n_O^2)^2}} \right]$$

$$\times \left[\left(\frac{n_X}{n_O} \right) \frac{1 - P - n_O^2}{1 - P - n_X^2} - \frac{1 - \varepsilon - n_x^2 - n_O^2}{1 - \varepsilon - n_x^2 - n_X^2} \right]^{-2} \tag{5.12}$$

Figures 4a and 4b show T_{OX}, T_{OO}, n_X^2, and n_O^2 plotted as a function of n_x for b = 0.7 and b = 1.1, respectively. P was taken to be 0.1. In Fig. 4a T_{OX} is zero for $n_x = 0$, increases to a maximum, and, then, decreases rapidly to zero at the point where $n_X^2 = 0$ ($n_x = n_{x\ cutoff} = 0.82$). The value $n_{x\ cutoff}$ corresponds to the point at which the extraordinary mode right-hand cutoff occurs at density P. For larger values of n_x the extraordinary mode is evanescent at this density, and T_{OX} is purely imaginary. When $b = |\Omega_e|/\omega > 1$ (see Fig. 4b), both modes propagate up to $n_x = [1 - P/(1 + b)]^{1/2} = 0.97$, at which point $n_O^2 = 0$ (the incident wave is parallel to the reflecting surface) and $T_{OX} = 0$.

Using the general expressions, we have calculated T_{OX} as a function of the polar angles of $\underset{\sim}{n}$ for the incident ordinary wave $\phi = \tan^{-1}(n_y/n_x)$, $\theta = \tan^{-1}(n_z/\sqrt{n_x^2 + n_y^2})$. Figure 5 shows three-dimensional (3-D) plots of T_{OX} versus θ and ϕ for various values of magnetic field strength $b = \Omega_e/\omega$. The plasma density chosen was appropriate for the surface plasma in EBT-I, $n_e = 2 \times 10^{11}/cm^3$ ($P = \omega_{pe}^2/\omega^2 = 0.05$, $\omega/2\pi = 18$ GHz), and ψ was taken to be 90° (i.e., the magnetic field is parallel to the reflecting surface). Notice that in each example a fraction approaching 1.0 of the energy in an incident wave can be mode converted at certain angles. Assuming an uncorrelated distribution of incident waves that is uniform in $\underset{\sim}{n}$ over the solid angle for which both waves propagate, we obtain an average fraction of ordinary mode power converted to extraordinary mode, $\langle T_{OX} \rangle$. As seen in Fig. 5, $\langle T_{OX} \rangle$ is very significant, being even larger than 0.5 for low magnetic field and in the range 0.3–0.5 for b > 1. In order to demonstrate the effect of the magnetic field being oblique to the reflecting surface, we have included

in Fig. 6 a set of plots having identical parameters to those in Fig. 5 except that ψ is now 60°. The surfaces in Fig. 6 are somewhat distorted from their counterparts in Fig. 5, and T_{OX} no longer vanishes at $\phi = \pi/2$. The averages $\langle T_{OX} \rangle$ for the oblique field are somewhat larger at low field ($b < 1$) and somewhat smaller at high field ($b > 1$) than the corresponding values for $\psi = 90°$. However, the average conversion efficiencies remain in the range $0.3 \lesssim \langle T_{OX} \rangle \lesssim 0.7$.

There are a number of factors which complicate the interpretation of these average T_{OX} results. First, let us consider the reflection/mode conversion process for angles near the right-hand cutoff when the magnetic field is weak ($b < 1$). Assume that both ordinary and extraordinary modes propagate but that n_x, n_y are near values such that $n_z^2 = 0$ for the extraordinary mode. So far, the plasma density has been assumed spatially constant. However, if the plasma is plane stratified with the density increasing away from the reflecting surface, then the upgoing mode converted extraordinary wave soon reaches the density of the right-hand cutoff for the given n_x, n_y. The extraordinary wave is reflected from the cutoff back to the conducting surface, where it is reconverted to a mixture of upgoing ordinary and extraordinary modes. The process is repeated with the secondary upgoing extraordinary wave until, ultimately, only ordinary mode energy can emerge at large distances from the conducting surface. Actually, neither the density nor the magnetic field in EBT is plane stratified and, of course, the magnetic field lines are not straight, so the simple model discussed here cannot be used to predict the energy flow far from the wall surface. In fact,

ray-tracing studies have shown that extraordinary mode energy originating near the surface can penetrate deep into the plasma for all but the most grazing angles of injection.

Another interesting situation arises when the angle of the incident ordinary wave is so large that the converted extraordinary mode is evanescent. Consider, for example, the case shown in Fig. 4a with $n_x > n_{x\ \text{cutoff}}$. Provided n_x is less than the ordinary mode cutoff, the ordinary mode can propagate to the surface and be partially reflected. The reflected ordinary wave cannot, however, carry away the total wave energy. The remaining energy goes to excite extraordinary polarization, which, being evanescent, does not transport energy. The oscillating field of the extraordinary mode must build up until ponderomotive effects push the plasma away from the wall, which leaves a thin layer where the extraordinary mode does propagate. With a density gradient established, the propagating extraordinary mode is reflected back to the surface (as in the previous discussion). The final result is therefore a modification of the density profile near the wall with all incident wave energy returning as ordinary mode.

The two effects just described tend to reduce the conversion of ordinary to extraordinary mode for nearly grazing angles of incidence. This, however, is a quantitatively small effect, and we still expect average conversion efficiencies in the vicinity of 0.5 to prevail. In addition, there are other processes, not included in the simple wall reflection model, which tend to enhance conversion between modes. Most notable is the internal mode coupling produced by density and magnetic field variations. When the plasma frequency and cyclotron frequency are

small compared to the wave frequency, the ordinary mode and extraordinary mode are nearly degenerate. If the plasma is uniform, there is no coupling. Or, if the variations in equilibrium quantities are of a sufficiently large scale length, the fields are well described by geometrical optics, and coupling between modes is exponentially small despite the near degeneracy. However, if $n_e(\underset{\sim}{x})$ and $\underset{\sim}{B}(\underset{\sim}{x})$ have small scale length fluctuations, geometrical optics breaks down, and significant conversion can occur. The details of this process are described by a complicated set of coupled mode equations [2,7] and depend sensitively on the difference between the refractive index of the two modes $\Delta n = n_0 - n_x$, the scale length of equilibrium variations L, the angle between $\underset{\sim}{n}$ and $\underset{\sim}{B}$, and the angle between $\underset{\sim}{B}$ and the direction of the equilibrium gradients. A rough criterion [8] for the geometrical optics results to be valid is that the variation in local refractive index for one of the modes within one wavelength λ (dn_j/ds) must be small compared to the refractive index difference Δn:

$$\frac{\lambda}{L} << \frac{\Delta n}{n_j} \tag{5.13}$$

Probe measurements of the EBT surface plasma have indicated that the density is fairly flat, at least in the midplane region. However, unstable fluctuations have been observed in the surface plasma [9] for which Eq. (5.13) is certainly violated. Additional conversion between modes is therefore expected from this mechanism.

Finally, it should be noted that the EBT wall has a very irregular shape with numerous edges, corners, and intrusions. Waves incident on

these edges are diffracted rather than specularly reflected, resulting in an additional randomization of wave polarization.

As can be seen, significant conversion between ordinary mode and extraordinary mode occurs just due to specular reflection at the cavity walls. In addition, the above mentioned diffraction and fluctuation effects in the low density surface plasma tend to equipartition energy between the two modes. We therefore model the mode conversion rate coefficients ocurring in Eq. (2.6) as

$$\tau_{XO}^{j} = \int_{S_{wall}^{j}} d\sigma \int \frac{d^3k}{4\pi} \underset{\sim}{v}_g(\underset{\sim}{k}) t_{XO}(\underset{\sim}{x},\underset{\sim}{k})$$

$$= c \int_{S_{wall}^{j}} d\sigma \int \frac{d\Omega}{4\pi} \hat{k} \cdot \hat{n} t_{XO} = \beta^{j} \frac{c}{2} S_{wall}^{j} \qquad (5.14)$$

where we have again approximated $\underset{\sim}{v}_g = c\hat{k}$ and β^j is a wall-surface and angle-averaged conversion coefficient for region j. In most calculations we have chosen $\beta^j = 0.5$ although we have studied the effect of reducing β^j. Note that reciprocity ensures that β is the same for the $O \rightarrow X$ process as for the $X \rightarrow O$ process.

6. GEOMETRICAL PARAMETERS AND NUMERICAL ESTIMATES OF RATE COEFFICIENTS

Each of the rate coefficients discussed above depends upon the area of some resonant or wall surface. In order to obtain estimates of these geometrical quantities we made measurements from Fig. 7, which shows the cavity walls for EBT-I, as well as field lines and mod-B contours for a 3-D, finite-beta equilibrium. The measurements were then scaled to the actual size for EBT-I. Table I shows the surface area values used in the numerical calculations. Estimates for the volume of regions I and II that are necessary to calculate the total wave energy in each mode are also shown in Table I.

We are now able to obtain numerical estimates for the rate coefficients derived in the previous sections. These are presented in Table II. It can be seen that by far the fastest decay process for the ordinary mode is conversion to extraordinary mode, $\tau_{OX}^{I} + \tau_{OX}^{II} = 3.63 \times 10^{13}$ cm^3/s. The rates for absorption at the cyclotron resonance ($\alpha_O^{II} \lesssim 6.6 \times 10^{11}$ cm^3/s) and by the annulus ($\alpha_O^{I} \sim 4 \times 10^{11}$ cm^3/s) are more than an order of magnitude lower. The principal decay process for the extraordinary mode in region I is conversion to ordinary mode, which is much faster than either absorption by the annulus or tunneling processes. The extraordinary mode in region II is lost predominantly by absorption at the fundamental cyclotron resonance ($\alpha_X^{II} = 2.25 \times 10^{13}$ cm^3/s) although conversion to ordinary mode is competitive ($\tau_{XO}^{II} = 1.15 \times 10^{13}$ cm^3/s).

Table I. Surface area and volume estimates

Geometrical parameter	Numerical estimates
Area of fundamental resonance intersecting core, S_C^{II}	443 cm^2
Area of fundamental resonance intersecting surface plasma, S_S^{II}	1087 cm^2
Total area of fundamental resonance, S_R^{II} $(S_C^{II} + S_S^{II})$	1530 cm^2
Area of conducting wall bounding region I, S_{wall}^{I}	3.3×10^3 cm^2
Area of conducting wall bounding region II, S_{wall}^{II}	880 cm^2
Volume of region I, V_I	2.8×10^4 cm^3
Volume of region II, V_{II}	1.6×10^4 cm^3
Volume of region II with zone between the right-hand cutoff and cyclotron resonance excluded, V'_{II}	8.6×10^3 cm^3

Table II. Numerical values for rate coefficients

Rate coefficients	Numerical values (cm^3/s)
$\alpha_X^{II} = \frac{c}{2} S_R^{II}$	2.25×10^{13}
$\alpha_O^{II} = C\langle f\rangle S_C^{II}$	$\langle f\rangle 1.33 \times 10^{13}$ $\begin{cases} \Rightarrow 0, \text{ where } \langle f\rangle = 0 \\ \Rightarrow 6.6 \times 10^{11}, \text{ where } \langle f\rangle = 0.05 \end{cases}$
$\alpha_X^I = g_x \alpha_x$	1.5×10^{12}
$\alpha_O^I = (1 - g_x)\alpha_A$*	5.0×10^{11}
$\gamma_T = \lvert T\rvert^2 \frac{c}{2} S_S^{II}$	$\lvert T\rvert^2 1.63 \times 10^{13}$ $\begin{cases} \Rightarrow 0, \text{ where } \lvert T\rvert^2 = 0 \\ \Rightarrow 2.45 \times 10^{12}, \text{ where } \lvert T\rvert^2 = 0.15 \end{cases}$
$\gamma_A = \lvert T\rvert^2(1 - \lvert T\rvert^2)\frac{c}{2} S_S^I$	$\lvert T\rvert^2(1 - \lvert T\rvert^2)1.33 \times 10^{13}$ $\begin{cases} \Rightarrow 0, \text{ where } \lvert T\rvert^2 = 0 \\ \Rightarrow 2.08 \times 10^{12}, \text{ where } \lvert T\rvert^2 = 0.15 \end{cases}$
$\tau_{OX}^I = \beta^I \frac{c}{2} S_{wall}^I$	$4.95 \times 10^{13}\beta^I$ or 2.48×10^{13}, where $\beta^I = 0.5$
$\tau_{OX}^{II} = \beta^{II} \frac{c}{2} S_{wall}^{II}$	$2.30 \times 10^{13}\beta^{II}$ or 1.15×10^{13}, where $\beta^{II} = 0.5$

*Using $\alpha_A = 2.0 \times 10^{13}$ cm^3/s, obtained from model with $f_A = 0.25$, and $g_x = 0.75$.

7. RESULTS

One of the primary objectives of this analysis is to obtain estimates of the microwave power deposited in each plasma component. The power absorbed by the core plasma P_C consists of the extraordinary mode power in region II absorbed along that portion of the resonant surface which intercepts the core plasma S_C^{II} (see Fig. 1) as well as any ordinary mode absorbed at the fundamental resonance

$$P_C = \frac{S_C^{II}}{S_R^{II}} \alpha_X^{II} W_X^{II} + \alpha_O^{II} W_O \tag{7.1}$$

The power deposited in the surface plasma P_S consists of the extraordinary mode power in region II absorbed along that portion of the resonant surface which intercepts the surface plasma S_S^{II} and any extraordinary mode power absorbed from region I through Budden tunneling

$$P_S = \frac{S_S^{II}}{S_R^{II}} \alpha_X^{II} W_X^{II} + \gamma_A W_X^{I} \tag{7.2}$$

Absorption of the ordinary mode in the surface plasma is entirely negligible. The power deposited in the annulus P_A is

$$P_A = \alpha_X^{I} W_X^{I} + \alpha_O^{I} W_O \tag{7.3}$$

For simplicity we have treated the annulus as lying entirely in region I (as drawn in Fig. 1). Undoubtedly, some hot electrons do pass through the fundamental cyclotron resonance, and some of the microwave power

that is absorbed at the fundamental resonance goes directly to the annulus. However, experiments in several hot electron ring devices have shown that the bulk of the annulus is confined to an axial segment whose length is roughly equal to the ring radius and which does not extend to the cyclotron resonance layer.

Equations (7.1) and (7.2) give a simple but very important result. To the extent that absorption of ordinary mode and tunneling processes are negligible ($\alpha_O^{II} = \gamma_A = 0$), the ratio of P_C to P_S is just S_C^{II}/S_S^{II}. For the EBT-I case we have

$$\frac{P_C}{P_S} = \frac{S_C^{II}}{S_S^{II}} = 0.41 \qquad (7.4)$$

Coupling this with the observation that $P_A \sim 0.25P_{TOT}$ where P_{TOT} is the total microwave power injected, we have

$$P_C = 0.22P_{TOT}$$

$$P_S = 0.53P_{TOT}$$

$$P_A = 0.25P_{TOT}$$

This approximate partitioning of microwave power is borne out in more detailed calculations presented below. In particular, we find that in each case large amounts of power are absorbed by the low density surface plasma despite its comparatively low density and temperature. It should be emphasized that the calculations assume that the flux of extraordinary mode energy is uniform over the fundamental resonant surface. Since the source of extraordinary mode energy is mode conversion at the cavity

wall, it is to be expected that any deviation from uniform illumination of the resonant surface will consist of a higher flux in the outer surface plasma than in the core plasma. The estimates obtained for P_C/P_S can therefore be considered an upper bound.

The power balance equations [Eqs (2.7)-(2.9)] determine the energy densities in terms of the rate coefficients and the injected power. Solving Eq. (2.7) for W_X^I gives

$$W_X^I = \frac{P_X + \tau^I W_O^I}{\alpha_X^I + \tau^I + \gamma_A + \gamma_T} \tag{7.5}$$

Using this in Eq. (2.8) gives

$$W_X^{II} = \frac{\left(\tau^{II} + \dfrac{\tau^I \gamma_T}{\alpha_X^I + \tau^I + \gamma_A + \gamma_T}\right) W_O + \dfrac{\gamma_T}{\alpha_X^I + \tau^I + \gamma_A + \gamma_T} P_X}{\alpha_X^{II} + \tau^{II}} \tag{7.6}$$

Using these equations in Eq. (2.9) to eliminate W_X^I and W_X^{II}, we obtain

$$W_O = \frac{P_O + \dfrac{P_X}{\alpha_X^I + \tau^I + \gamma_T}\left(\tau^I + \dfrac{\gamma_T \tau^{II}}{\alpha_X^{II} + \tau^{II}}\right)}{\alpha_O^I + \alpha_O^{II} + \tau^I\left(1 - \dfrac{\tau^I + \dfrac{\gamma_T \tau^{II}}{\alpha_X^{II} + \tau^{II}}}{\alpha_X^I + \tau^I + \gamma_A + \gamma_T}\right) + \tau^{II}\left(1 - \dfrac{\tau^{II}}{\alpha_X^{II} + \tau^{II}}\right)} \tag{7.7}$$

The subscripts were dropped from τ_{OX}^j and τ_{XO}^j because of assumed reciprocity in mode conversion.

At this point only P_O and P_X remain unspecified. In EBT-I the microwaves are injected at the midplane of each cavity by means of rectangular, dominant mode waveguides. It has been experimentally observed that plasma parameters are somewhat better and the power reflected back toward the klystrons is lower when the waveguides are oriented with the $\underset{\sim}{E}$ plane (short dimension) along the magnetic field. Although the relative division between ordinary and extraordinary mode power has not been measured, we expect that in this configuration the ordinary mode is preferentially excited. We therefore model the injected power as

$$\begin{aligned} P_X &= f_X P_{TOT} \\ P_O &= (1 - f_X) P_{TOT} \end{aligned} \tag{7.8}$$

where the fraction of injected power going into the extraordinary mode f_X is assumed small. The results are found to be only weakly dependent on f_X for $0 \leq f_X < 0.5$, the widest credible range.

We now consider the situation in which the fraction of injected power deposited in the annulus is constrained to be a fixed fraction f_A of the injected power by setting $P_A = f_A P_{TOT}$. Using Eqs (3.9), (7.4), (7.7), and (7.8) in Eq. (7.3), we obtain a quadratic equation for the overall annulus absorption coefficient α_A:

$$g_X(1 - g_X)(1 - f_A)\alpha_A^2 + \Bigg[(1 - f_A)\tau^I + (1 - g_X)(\gamma_A + \gamma_T)(1 - f_X - f_A)$$

$$+ g_X\left(\alpha_0^{II} + \frac{\alpha_X^{II}\tau^{II}}{\alpha_X^{II} + \tau^{II}}\right)(f_X - f_A) + \frac{(1 - g_X)\gamma_T\tau^{II}}{\alpha_X^{II} + \tau^{II}}\Bigg]\alpha_A$$

$$- f_A\Bigg[\tau^I\left(\alpha_0^{II} + \gamma_A + \frac{\alpha_X^{II}\tau^{II}}{\alpha_X^{II} + \tau^{II}}\right)$$

$$+ (\gamma_A + \gamma_T)\left(\alpha_0^{II} + \frac{\alpha_X^{II}\tau^{II}}{\alpha_X^{II} + \tau^{II}}\right)\Bigg] = 0 \qquad (7.9)$$

Because of the sign of the last term, only one of the solutions for α_A is positive (i.e., physical).

Solving Eq. (7.9) and using the results in Eqs (7.1)-(7.7), we obtain the fraction of microwave power deposited in the core plasma P_C/P_{TOT}. In Fig. 8 f_A has been fixed at 0.25 and the variation of P_C/P_{TOT} with the Budden tunneling coefficient $|T|^2$ is shown for various values of f_X, g_X, α_0^{II}, and β^I. The extreme range of credible values is included for each of these parameters: the fraction of injected power going into the ordinary mode (f_X = 0, 0.5), the relative opacity of the annulus to extraordinary versus ordinary mode [g_X = 0.5 (solid curves); g_X = 1.0 (dashed curves)], and the ordinary mode absorption by the core plasma (α_0^{II} = 0, 0.05). In Fig. 8a the mode conversion efficiencies β^I, β^{II} are taken to be 0.5, which we consider the most plausible choice. We see that when α_0^{II} is neglected increasing $|T|^2$ from 0.0 to 0.15 reduces the fraction of power deposited in the core from 25% to about 17%, a comparatively small change. The value $|T|^2$ = 0.15 must be considered an extreme value obtainable only with very low surface plasma

density. The effect of increasing α_O^{II} to 0.05 (also an extreme value for EBT-I) is to increase P_C/P_{TOT} from about 22% to 25% at $|T|^2 = 0$ and to increase P_C/P_{TOT} to a lesser extent at higher $|T|^2$. It is clear that the results are very insensitive to the choice of f_X and g_X. This is indicative of the dominant role played by the equipartition between ordinary and extraordinary modes upon wall reflection. Even in the case $f_X = 0$ (i.e., no extraordinary mode energy injected), the extraordinary mode energy density W_X^I is found to be nearly as large as the ordinary mode energy density W_O.

In Fig. 8b the mode conversion efficiencies were reduced to $\beta^I = \beta^{II} = 0.1$. In this case the choice of f_X and g_X has a much larger influence, but the maximum effect on P_C/P_{TOT} is still only a few percent. Reducing β^j increases the number of passes of a ray through the plasma before it is mode converted. This in turn enhances the effect of tunneling and ordinary mode absorption compared to extraordinary mode absorption at the fundamental cyclotron resonance. Nevertheless, a decrease in β^j by a factor of 5 results in an increase in P_C/P_{TOT} at $|T|^2 = 0$ of only about 7% when the maximum credible value is used for α_O^{II}. Since P_A/P_{TOT} is constant in Fig. 8, the power deposited in the surface plasma can be determined directly from P_C/P_{TOT}: $P_S/P_{TOT} = 1 - 0.25 - P_C/P_{TOT}$.

Some discussion is in order concerning the interpretation of these curves. We certainly do not suggest that the annulus adjusts itself as parameters are varied so as to absorb a constant fraction of the input power. However, the experiment indicates that there is an operating point such that f_A is about 0.25. This point must therefore lie within

the bounds of the curves in Fig. 8. Since P_C/P_{TOT} is insensitive to the other parameters of the model, we can say with reasonable certainty that 18-25% of the injected microwave power is absorbed in the core plasma.

Figures 9 and 10 show the fraction of power deposited in each plasma component when α_A rather than f_A is fixed. We have set $\alpha_A = 2.0 \times 10^{12}$ cm^3/s, which gives $P_A/P_{TOT} = 0.25$ for an intermediate choice of parameter values: $f_X = 0.25$, $g_X = 0.75$, $|T|^2 = 0.025$, $\alpha_O^{II} = 0.025$, and $\beta^j = 0.5$. In Fig. 9 the fraction of power going into the core component is plotted as a function of $|T|^2$ for the same ranges of g_X, f_X, α_O^{II}, and β^j used in Fig. 8a. It can be seen that the behavior of P_C/P_{TOT} is essentially the same as when f_A is fixed.

Figure 10 shows how the partitioning of deposited energy changes with the overall annulus absorption coefficient α_A. Figures 10a-10d show the effect of $\alpha_A = 1$, 2, 4, and 8×10^{12} cm^3/s, respectively. One sees a dramatic tradeoff of surface plasma heating to annulus heating but a much smaller effect on core heating. Although α_A is varied by a factor of 7 and the power deposited in the annulus changes by almost a factor of 4, the power deposited in the core is decreased by less than a factor of 2.

Using this model it is also possible to estimate a value for the microwave Q of EBT. The total stored electromagnetic wave energy can be expressed as

$$W_{TOT} = V_I W_X^I + V_{II} W_X^{II} + (V_I + V_{II}) W_O \tag{7.10}$$

so that the stored energy divided by the energy dissipated per cycle is

$$Q = f_\mu \times \frac{W_{TOT}}{P_{TOT}} \tag{7.11}$$

where f_μ is the microwave frequency. Using the volumes given in Table I and parameters similar to those used in Figs 5-7, one finds Q values in the range $125 \lesssim Q \lesssim 200$. These values seem quite large for such a dissipative system as EBT. However, one must bear in mind that EBT is an extremely large device compared to the wavelength. Extraordinary mode energy is very rapidly absorbed at the fundamental resonance, but a typical wave must travel many wavelengths to be absorbed. There is therefore a large inventory of stored wave energy in the form of propagating waves. It must be admitted that for a device such as EBT, Q is not experimentally measurable and hence not a very useful concept. Standing-wave-ratio measurements are difficult to make and are probably impossible to interpret, and since the absorbing nature of EBT changes with the wave frequency (i.e., the location of resonant zones, cutoffs, and plasma parameters), the measurement of the absorption line width in frequency would be meaningless.

8. CONCLUSIONS

In this paper we have collected a number of previous results on the various sources and sinks of ordinary and extraordinary mode radiation and have developed a comprehensive, although very approximate, model for the propagation and absorption of microwaves in EBT devices. The model has been applied in detail to the EBT-I device. We find that the dominant processes are the conversion between plasma eigenmodes and the absorption of the extraordinary mode at the fundamental cyclotron resonance. Absorption by the relativistic electron annulus is a weaker process. The modifications due to Budden tunneling, ordinary mode absorption, and polarization of the injected waves are very minor.

Perhaps the most significant result of the model is that in EBT-I a large fraction of the injected microwave power is deposited in the poorly confined surface plasma. This is so even though the density and temperature of the surface plasma are considerably less than those of the core plasma. The core plasma in EBT-I tends to absorb about 20% of the injected microwave power despite wide variations in the model parameters. The partitioning of energy between the surface and the core plasma is largely determined by the geometrical sizes of the fundamental resonant zone surfaces that intercept the surface and core plasmas, respectively. The partitioning of energy between the annulus and the other plasma components is determined by a competition for extraordinary mode energy to be absorbed by the annulus or to be mode converted to ordinary mode in the low magnetic field region. A result not at all obvious is that the amount of power deposited in the core plasma is largely independent of the core density and temperature.

There actually exists some experimental confirmation of the results of this model. Of course, the annulus absorption model used in the $f_A = 0.25$ calculations is based on experimental data and does not constitute confirmation. However, the estimate for α_A of about 1.2×10^{12} cm^3/s predicted using preliminary results of the relativistic absorption code agrees well with the value of α_A obtained from the fixed f_A model ($\alpha_A \sim 2 \times 10^{12}$ cm^3/s). Also, the value of P_A/P_{TOT} predicted using the a priori model is in reasonable agreement with the experimental estimate ($0.2 \lesssim P_A/P_{TOT} \lesssim 0.3$). Recently, estimates of power balance in EBT-I and EBT-S have been made using experimental data [10]. For these estimates the particle confinement time τ_P, which can be measured with fair accuracy, was related to the energy confinement time τ_E using neoclassical transport arguments. The power balance $P_C = (3/2)nT_e/\tau_E$ then yielded P_C/P_{TOT} in the range 0.13-0.27, which just brackets the results of the theoretical power balance model.

There are a number of conceivable experiments that could test the assumptions and results of this model. Most notably, measurements of the relative microwave field strengths at various points in the cavity could test the validity of assuming a uniform energy density and isotropic propagation. Measurements of the relative microwave field strength components parallel and perpendicular to the magnetic field would verify the ratios of W_X^I/W_O and W_X^{II}/W_O predicted by the model. Measurement of the absolute microwave field strength could be used to determine the magnitudes of W_X^I, W_X^{II}, and W_O.

This power balance model can certainly be applied to EBT-S. As far as this power balance model is concerned there is little difference

between EBT-I and EBT-S. The annuli in EBT-S form at a slightly smaller radius, which affects P_C/P_S. The opacity of the annulus is also expected to be somewhat greater in EBT-S. We have not emphasized EBT-S in the present work pending further development of the fully relativistic annulus absorption modeling and experimental results on the annulus energy lifetime in EBT-S. It may also be possible to extend the analysis to EBT-P and larger devices although the strong absorption of the ordinary mode at the fundamental resonance in hotter, denser devices calls into question the assumption of uniform energy density and isotropy of wave propagation. Ideas developed here should also be applicable to propagation of short wavelength radiation in other large, intricately shaped devices. A very relevant problem to attack would be the generation, depolarization, and absorption of synchrotron radiation in tokamaks and mirrors.

ACKNOWLEDGMENTS

The author would like to thank Professor Harold Weitzner who first suggested a statistical approach to the wave propagation problems in EBT and R. G. Goldfinger who was a collaborator on the ray tracing studies. Numerous valuable discussions were also held with R. A. Dandl, G. R. Haste, H. O. Eason, and T. L. White.

REFERENCES

[1] BATCHELOR, D. B., GOLDFINGER, R. C., Nucl. Fusion 20 (1980) 403.

[2] BATCHELOR, D. B., Plasma Phys. 22 (1980) 41.

[3] WEITZNER, H., BATCHELOR, D. B., Phys. Fluids 23 (1980) 1359.

[4] BATCHELOR, D. B., GOLDFINGER, R. C., A Theoretical Study of Electron Cyclotron Heating in ELMO Bumpy Torus, Oak Ridge National Lab. Rep. ORNL/TM-6992 (1979).

[5] BAITY, F. W., Jr., BECKER, M. C., CARPENTER, K. H., COBBLE, J. A., EASON, H. O., et al, Summary of EBT-I Experimental Results, Oak Ridge National Lab. Rep. ORNL/TM-6457 (1978).

[6] BATCHELOR, D. B., GOLDFINGER, R. C., WEITZNER, H., Bull. Am. Phys. Soc. 25 (1980) 964.

[7] BUDDEN, K. G., Radio Waves in the Ionosphere, Cambridge University Press, Cambridge (1961).

[8] GINSBURG, V. L., The Propagation of Electromagnetic Waves in Plasmas, 2nd Ed., Pergamon Press, Oxford (1970).

[9] KOMORI, A., Plasma Fluctuation Measurements in ELMO Bumpy Torus, Oak Ridge National Lab. Rep. ORNL/TM-7530 (1981).

[10] COLCHIN, R. J., SHEFFIELD, J., Bull. Am. Phys. Soc. 25 (1980) 831.

FIGURE CAPTIONS

Fig. 1. Cross section of a sector of EBT-I showing the three plasma components (core, surface, and annulus) and the two microwave propagation regions (I and II) defined for the power balance model. S_C^{II} and S_S^{II} are the surface areas of the fundamental cyclotron resonance zone intercepting the core and surface plasma components, respectively.

Fig. 2. Fraction of ordinary mode energy absorbed in a parallel stratified plasma versus injected value of n_x.

Fig. 3. Geometry for mode conversion upon reflection from a conducting wall.

Fig. 4. Mode conversion coefficients T_{OX}, T_{OO} and refractive indices n_X^2, n_O^2 as a function of n_x for magnetic field in the plane of incidence.

Fig. 5. Mode conversion coefficient T_{OX} versus polar angles of incidence θ, ϕ for various values of $b = \Omega_e/\omega$. The magnetic field is in the plane of the conducting wall.

Fig. 6. Mode conversion coefficient T_{OX} versus polar angles of incidence θ, ϕ for various values of $b = \Omega_e/\omega$. The magnetic field is at an angle $\psi = 60°$ with respect to a normal to the wall surface.

Fig. 7. Geometrical quantities used to estimate the power balance rate coefficients.

Fig. 8. Fraction of total power absorbed in core plasma versus Budden tunneling efficiency. The fraction of power absorbed in the annulus is fixed: $P_A/P_{TOT} = 0.25$.

Fig. 9. Fraction of total power absorbed in core plasma versus Budden tunneling efficiency. The annulus absorption coefficient is fixed: $\alpha_A = 2.0 \times 10^{12}$ cm^3/s.

Fig. 10. Partitioning of total absorbed power between surface core and annulus components versus Budden tunneling efficiency for various values of annulus absorption coefficient.

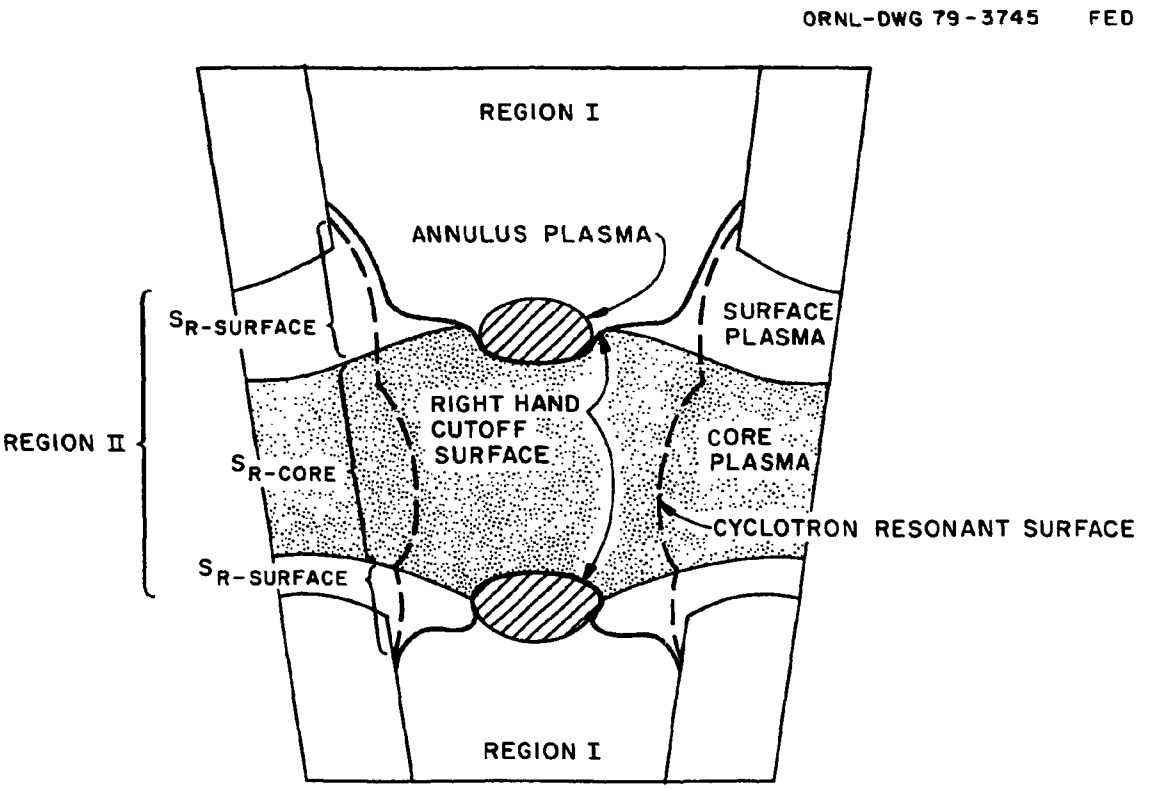
ORNL-DWG 79-3745 FED
REGION I
ANNULUS PLASMA
SURFACE PLASMA
$S_{R\text{-}SURFACE}$
REGION II
RIGHT HAND CUTOFF SURFACE
CORE PLASMA
$S_{R\text{-}CORE}$
CYCLOTRON RESONANT SURFACE
$S_{R\text{-}SURFACE}$
REGION I

Fig. 1

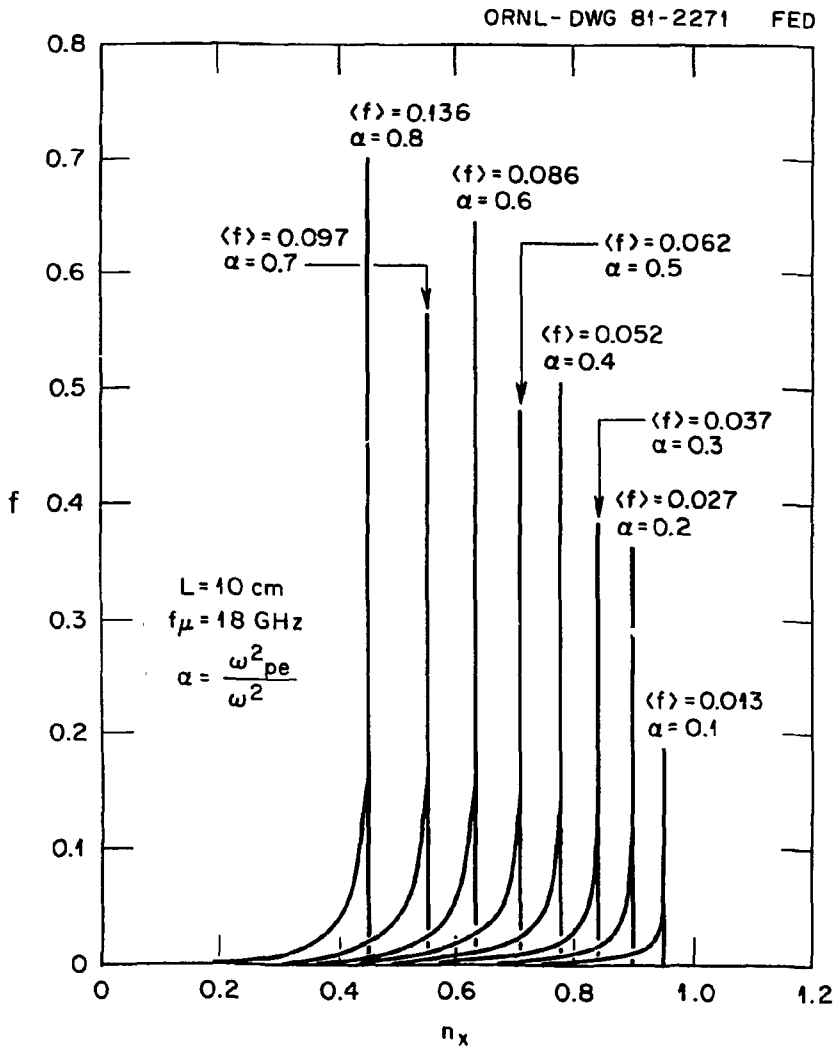
ORNL-DWG 81-2271 FED
⟨f⟩ = 0.136
α = 0.8
⟨f⟩ = 0.086
α = 0.6
⟨f⟩ = 0.097
α = 0.7
⟨f⟩ = 0.062
α = 0.5
⟨f⟩ = 0.052
α = 0.4
⟨f⟩ = 0.037
α = 0.3
⟨f⟩ = 0.027
α = 0.2
⟨f⟩ = 0.013
α = 0.1
L = 10 cm
fμ = 18 GHz
α = ω²pe / ω²
f
0.8
0.7
0.6
0.5
0.4
0.3
0.2
0.1
0
0
0.2
0.4
0.6
0.8
1.0
1.2
nx

Fig. 2

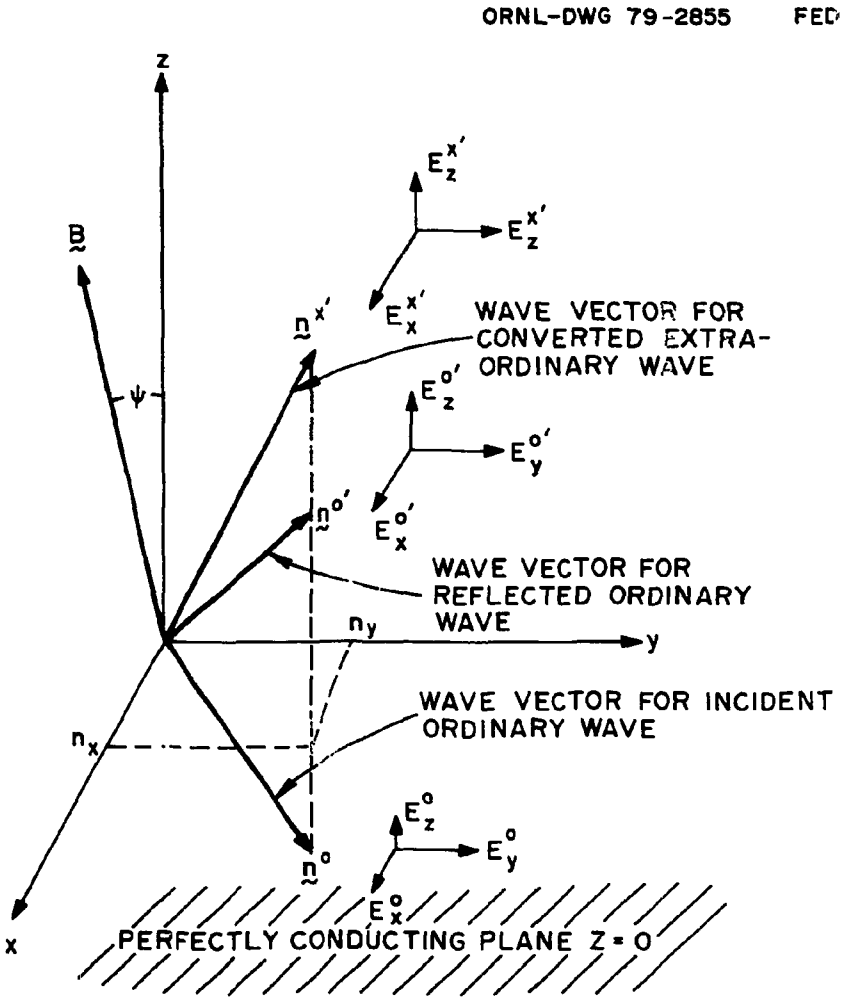
ORNL-DWG 79-2855 FED
z
B
ψ
$E_z^{x'}$
$E_z^{x'}$
$E_x^{x'}$
$n^{x'}$
WAVE VECTOR FOR CONVERTED EXTRA-ORDINARY WAVE
$E_z^{o'}$
$E_y^{o'}$
$n^{o'}$
$E_x^{o'}$
WAVE VECTOR FOR REFLECTED ORDINARY WAVE
n_y
y
WAVE VECTOR FOR INCIDENT ORDINARY WAVE
n_x
E_z^{o}
E_y^{o}
n^{o}
E_x^{o}
x
PERFECTLY CONDUCTING PLANE Z = 0

Fig. 3

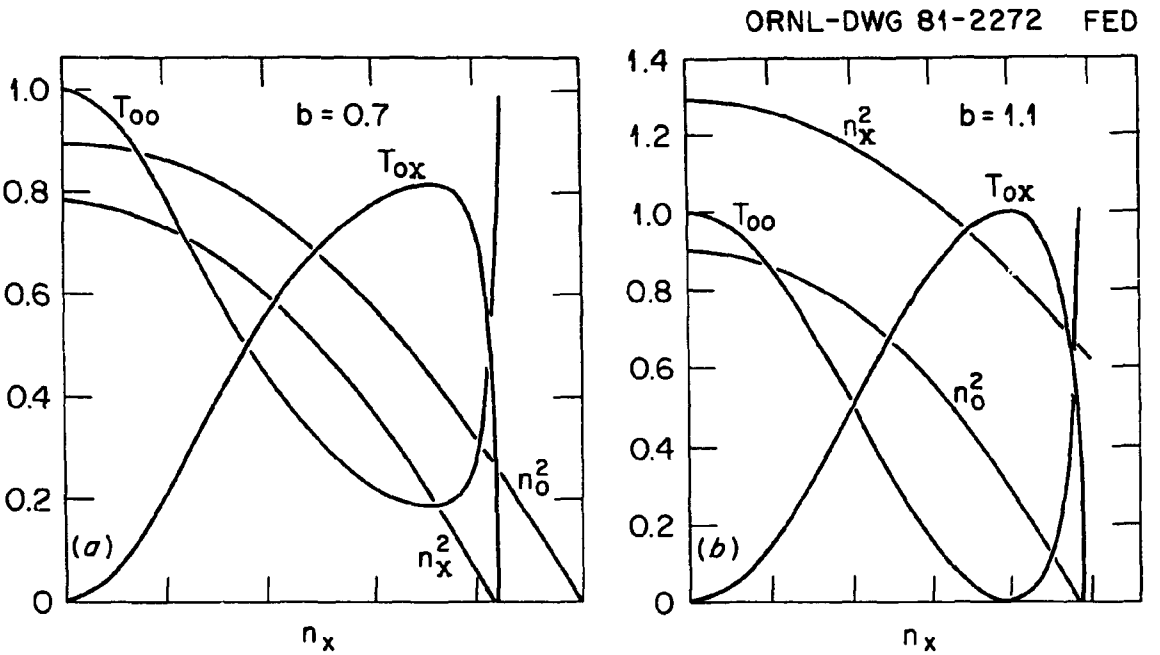
ORNL-DWG 81-2272 FED
1.0
0.8
0.6
0.4
0.2
0
T_{oo}
b = 0.7
T_{ox}
n_o^2
n_x^2
(a)
n_x
1.4
1.2
1.0
0.8
0.6
0.4
0.2
0
n_x^2
b = 1.1
T_{ox}
T_{oo}
n_o^2
(b)
n_x

Fig. 4

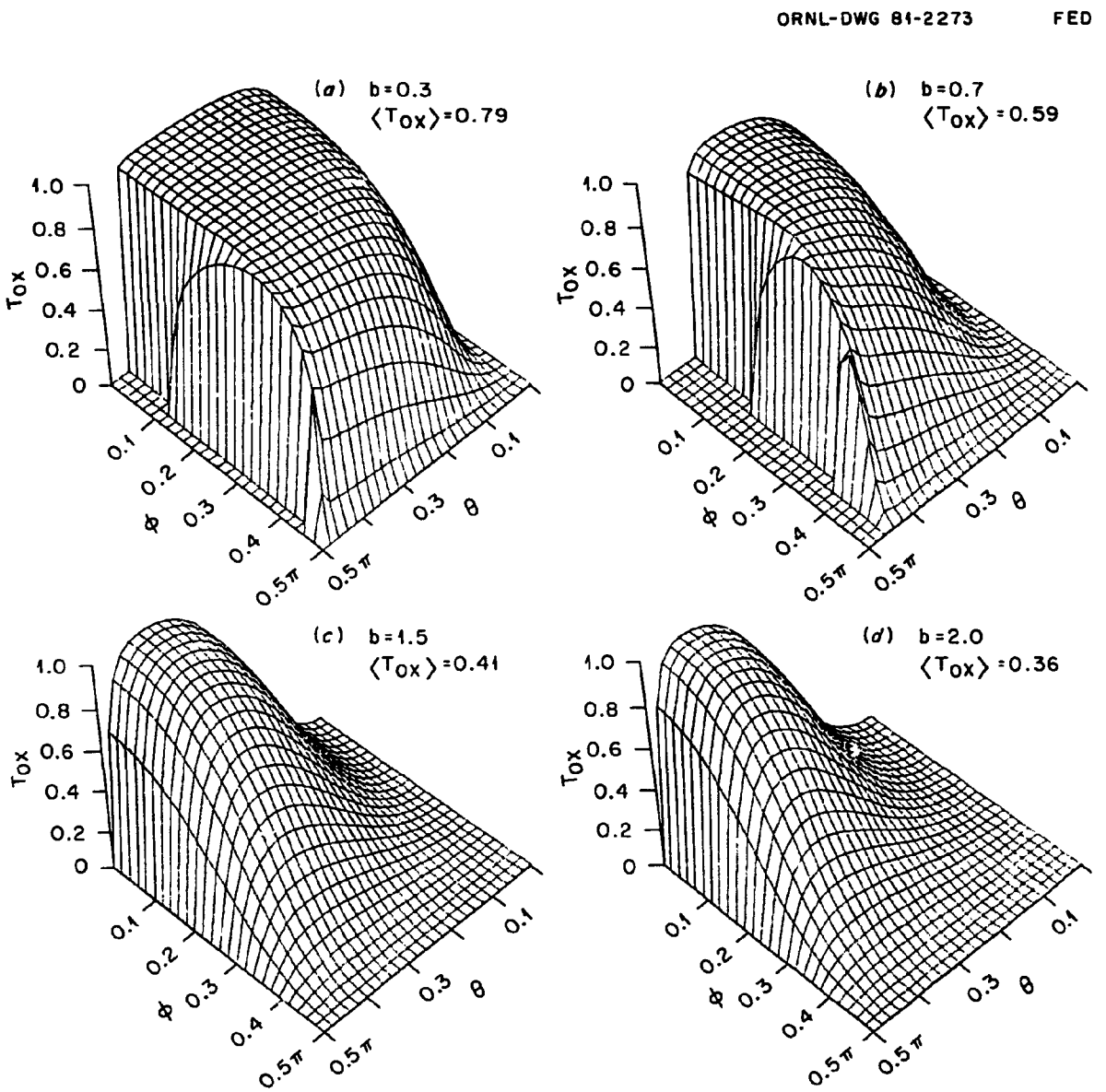
ORNL-DWG 81-2273 FED
(a) b=0.3
⟨Tox⟩=0.79
(b) b=0.7
⟨Tox⟩=0.59
(c) b=1.5
⟨Tox⟩=0.41
(d) b=2.0
⟨Tox⟩=0.36
Tox
1.0
0.8
0.6
0.4
0.2
0
0.1
0.2
0.3
0.4
0.5π
φ
θ

Fig. 5

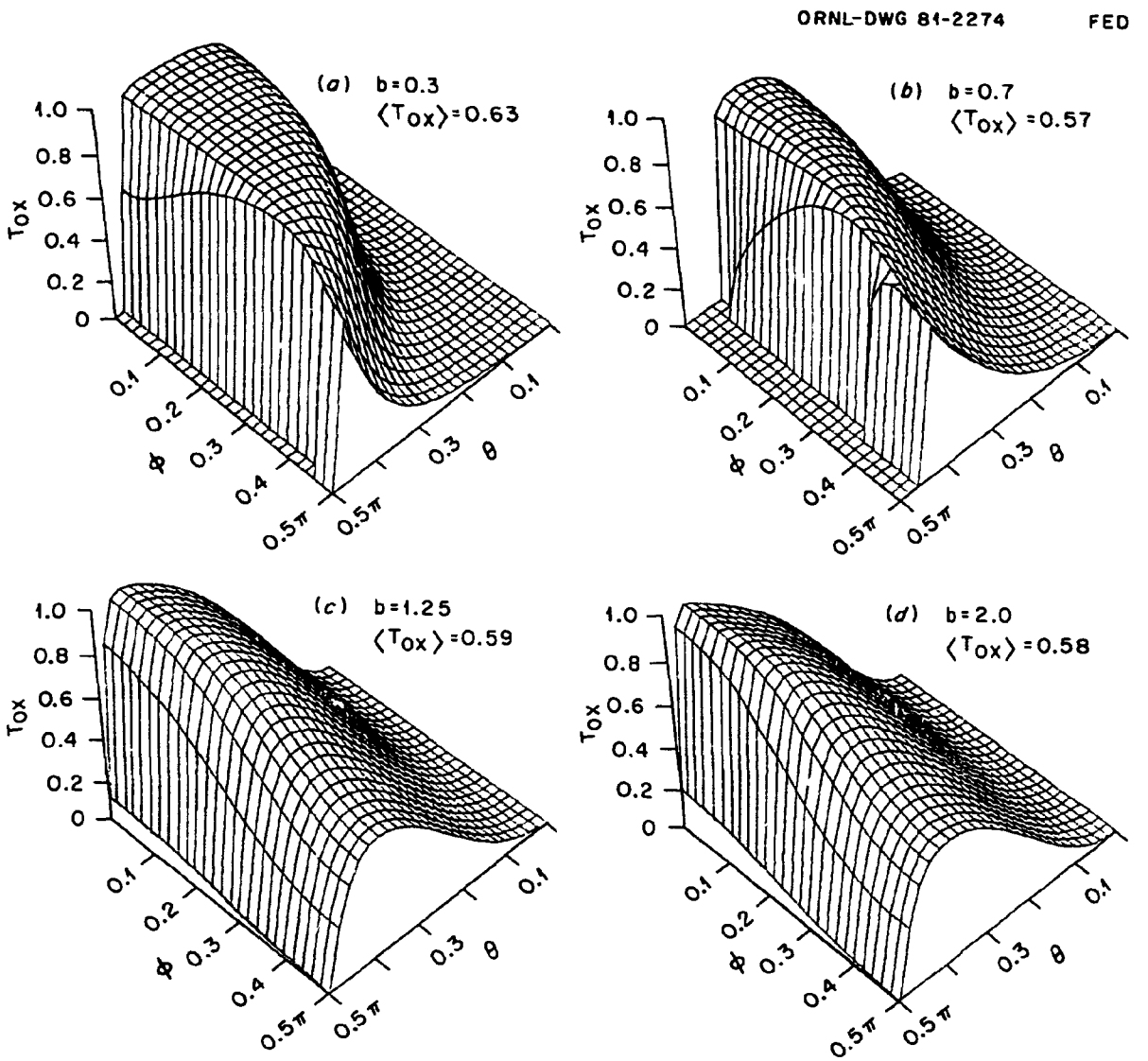
ORNL-DWG 81-2274 FED
(a) b=0.3
⟨Tox⟩=0.63
(b) b=0.7
⟨Tox⟩=0.57
(c) b=1.25
⟨Tox⟩=0.59
(d) b=2.0
⟨Tox⟩=0.58
Tox
1.0
0.8
0.6
0.4
0.2
0
0.1
0.2
0.3
0.4
0.5π
φ
θ

Fig. 6

GEOMETRY OF SINGULAR SURFACES IN EBT-I

ORNL-DWG 81-2275 FED

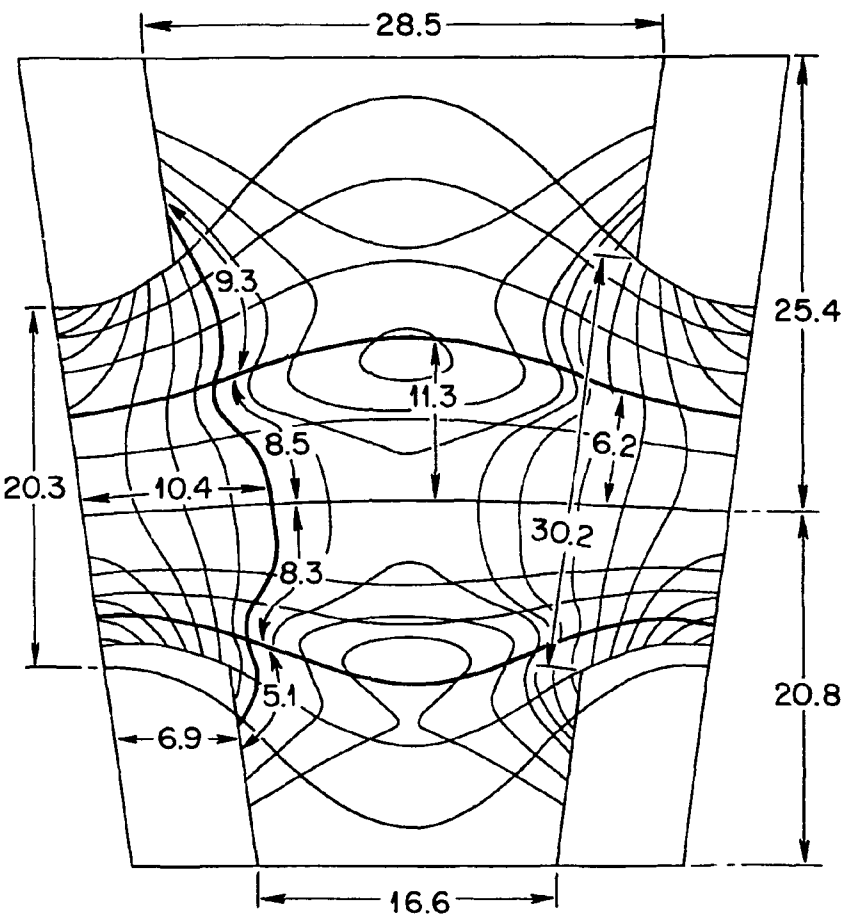

*DIMENSIONS IN (cm)

Fig. 7

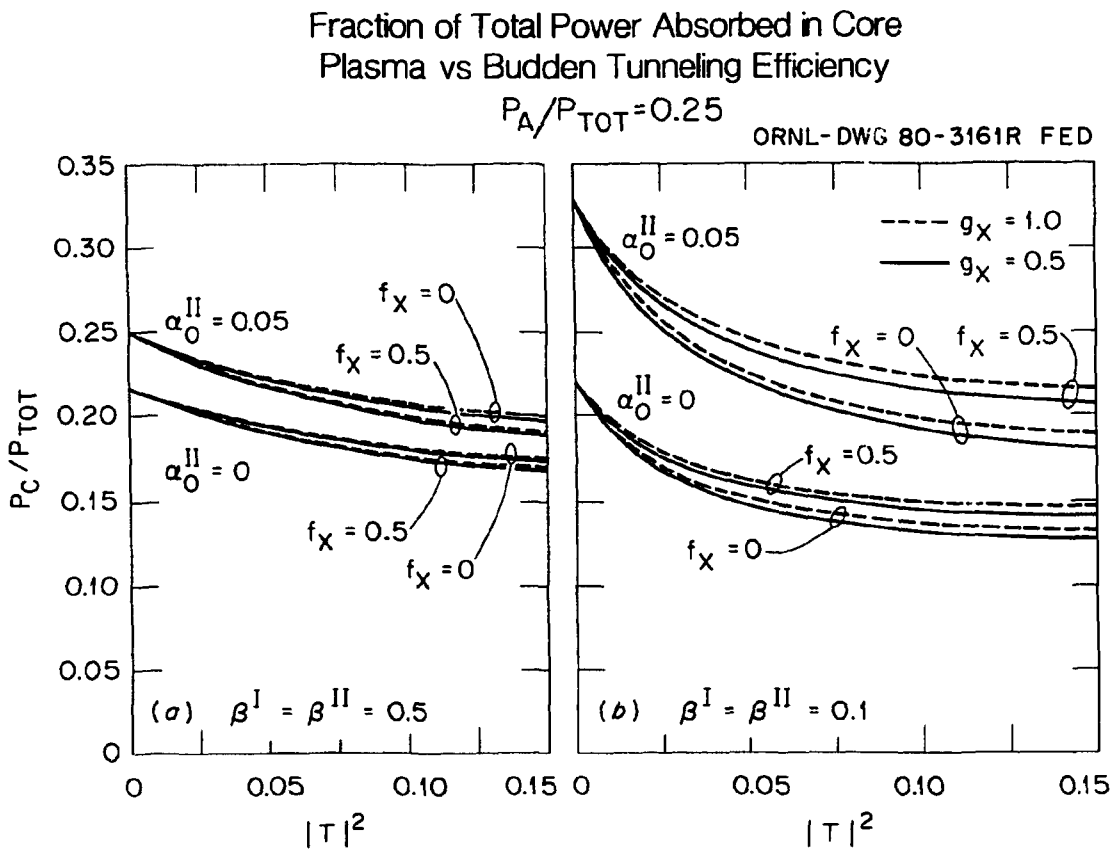
Fraction of Total Power Absorbed in Core
Plasma vs Budden Tunneling Efficiency
$P_A/P_{TOT}=0.25$
ORNL-DWG 80-3161R FED
P_C/P_{TOT}
$|T|^2$
$\alpha_0^{II}=0.05$
$\alpha_0^{II}=0$
$f_X=0$
$f_X=0.5$
$g_X=1.0$
$g_X=0.5$
(a) $\beta^I=\beta^{II}=0.5$
(b) $\beta^I=\beta^{II}=0.1$

Fig. 8

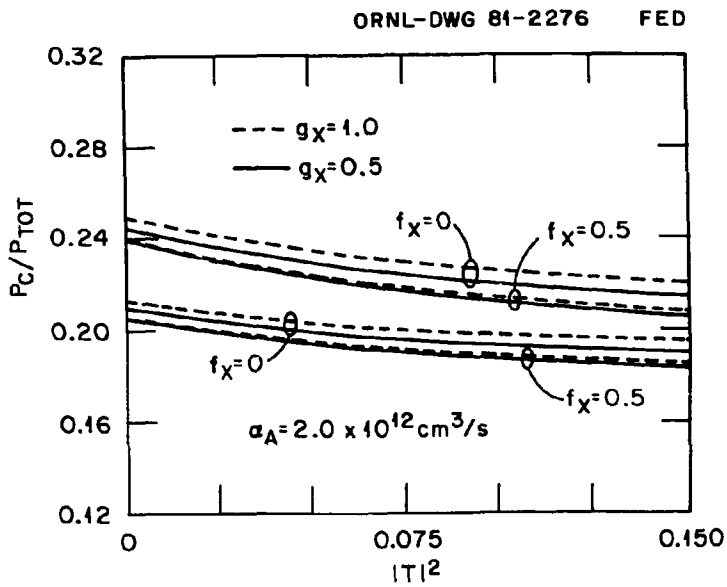
ORNL-DWG 81-2276 FED
0.32
0.28
0.24
0.20
0.16
0.12
P_C/P_{TOT}
g_X=1.0
g_X=0.5
f_X=0
f_X=0.5
f_X=0
f_X=0.5
α_A=2.0 x 10^{12} cm^3/s
0
0.075
0.150
$|T|^2$

Fig. 9

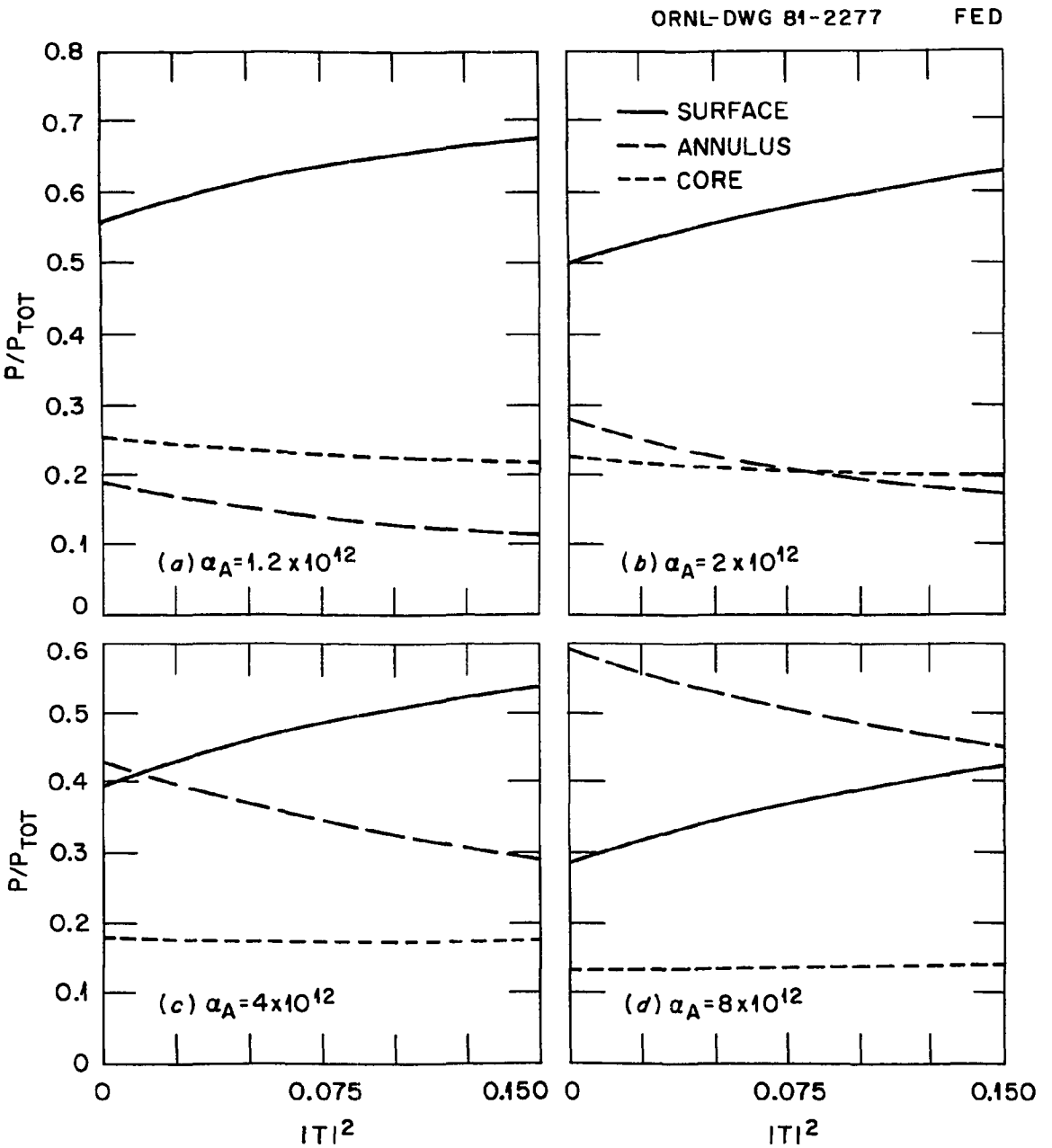
ORNL-DWG 81-2277 FED
SURFACE
ANNULUS
CORE
(a) $\alpha_A = 1.2 \times 10^{12}$
(b) $\alpha_A = 2 \times 10^{12}$
(c) $\alpha_A = 4 \times 10^{12}$
(d) $\alpha_A = 8 \times 10^{12}$
P/P_{TOT}
$|T|^2$
0
0.075
0.150
0.1
0.2
0.3
0.4
0.5
0.6
0.7
0.8

Fig. 10